2020

Estimation of self-sustained activity produced by persistent inward currents using firing rate profiles of multiple motor units in humans

Babak Afsharipour

Nagib Manzur

Jennifer Duchcherer

Keith K. Fenrich

Christopher K. Thompson

See next page for additional authors

Authors

Babak Afsharipour, Nagib Manzur, Jennifer Duchcherer, Keith K. Fenrich, Christopher K. Thompson, Francesco Negro, Katharina A. Quinlan, David J. Bennett, and Monica A. Gorassini

Estimation of self-sustained activity produced by persistent inward currents using firing rate profiles of multiple motor units in humans

Babak Afsharipour[1,7], Nagib Manzur[1], Jennifer Duchcherer[1,6], Keith F. Fenrich[5,6], Christopher K. Thompson[2], Francesco Negro[3], Katharina A. Quinlan[4], David J. Bennett[5,6] & Monica A. Gorassini[1,6,7]

[1]Department of Biomedical Engineering, University of Alberta, [2]Department of Health and Rehabilitation Sciences, Temple University, [3]Research Centre for Neuromuscular Function and Adapted Physical Activity "Teresa Camplani", Università degli Studi di Brescia, [4]Department of Biomedical and Pharmaceutical Sciences and George and Anne Ryan Institute for Neuroscience, University of Rhode Island, [5]Faculty of Rehabilitation Medicine, University of Alberta, [6]Neuroscience and Mental Health Institute, [7]Women and Children's Health Research Institute

Abstract: 249
Text: 15,028
Figures: 11
Supplemental Tables: 3

Key words: high-density surface EMG, motoneurons, persistent inward currents, tibialis anterior, recruitment threshold

Running title: Self-sustained firing in multiple human motor units

Corresponding Author:
Dr. Monica Gorassini, PhD
Department of Biomedical Engineering
Institute of Neuroscience and Mental Health
Women and Children's Health Research Institute
Faculty of Medicine and Dentistry
University of Alberta
Edmonton, AB CANADA T6G 0G2
monica.gorassini@ualberta.ca

NEW and NOTEWORTHY

A new method of estimating synaptic drive to multiple, simultaneously recorded motor units provides evidence that the portion of the depolarizing drive from persistent inward currents that contributes to self-sustained firing is similar across motoneurons of different sizes despite having different activation onsets with respect to firing threshold.

ABSTRACT

Persistent inward calcium and sodium currents (I_P) activated during motoneuron recruitment help synaptic inputs maintain self-sustained firing until de-recruitment. Here, we estimate the contribution of the I_P to self-sustained firing in human motoneurons of varying recruitment threshold by measuring the difference in synaptic input needed to maintain minimal firing once the I_P is fully activated compared with the larger synaptic input required to initiate firing prior to full I_P activation. Synaptic input to ≈20 dorsiflexor motoneurons simultaneously recorded during ramp contractions was estimated from firing profiles of motor units decomposed from high-density surface-EMG. To avoid errors introduced when using high-threshold units firing in their nonlinear range, we developed methods where the lowest-threshold units firing linearly with force were used to construct a composite (control) unit firing rate profile to estimate synaptic input to higher-threshold (test) units. The difference in the composite firing rate (synaptic input) at the time of test unit recruitment and de-recruitment ($\Delta F = F_{recruit} - F_{de\text{-}recruit}$) was used to measure I_P amplitude that sustained firing. Test units with recruitment thresholds 1-30% of maximum had similar ΔFs, which likely included both slow and fast motor units activated by small and large motoneurons, respectively. This suggests that the portion of the I_P that sustains firing is similar across a wide range of motoneuron sizes. Higher-threshold units had more prolonged accelerations in firing rate at the onset of recruitment compared to lower-threshold units, likely reflecting I_P activation closer to firing onset in the higher-threshold units, but well before firing onset in the lower-threshold units.

INTRODUCTION

Low voltage-activated persistent inward currents (I_P) flowing through $Ca_V1.2/1.3_s$ and $Na_V1.2/1.6$ ion channels amplify and prolong the firing behaviour of motoneurons in response to synaptic inputs, slowly activating over a relatively wide voltage range (≈10 mV) near the firing threshold (Binder et al. 2020; Carlin et al. 2000; Hounsgaard et al. 1988; Johnson et al. 2017; Li et al. 2004). The functional contribution of I_P and the depolarization, or plateau potential, it produces can be observed from the discharge behaviour of motoneurons in response to an increasing and decreasing synaptic current produced, for example, by slow triangular force contractions or graded sensory stimulation in both humans (Gorassini et al. 2002a; Gorassini et al. 1998; Kiehn and Eken 1997) and animals (Bennett et al. 1998b; Bennett et al. 2001a; Gorassini et al. 1999; Hounsgaard et al. 1988). The firing rate profiles of pairs of motor units during such contractions have been used to measure the potential contribution of I_P to self-sustained firing in human motoneurons (Gorassini et al. 2002a), although as we detail below this approach has limitations, including only allowing for the quantification of the I_P activated during firing, and not subthreshold to firing, inherently leading to an underestimation of the overall I_P in some motoneurons.

To understand these limitations and develop improved methods of I_P estimation, we start by outlining the basis for estimating the contribution of I_P to self-sustained firing from the firing profiles of motoneurons previously developed from animal studies. When a cat motoneuron is activated with synaptic inputs during a slow muscle stretch, the activation of the I_P always begins below the firing threshold of the motoneuron (Fig. 1A iv green trace) (Bennett et al. 1998b). In this example, the contribution of the I_P is inferred from the membrane (plateau) potential revealed when spikes are blocked. The activation of the I_P continues over a wide voltage range up to or sometimes after firing is initiated, producing an acceleration of the membrane depolarization just prior to firing (green arrow in Fig. 1A iv). This accelerated depolarization can produce a high firing rate at recruitment and sometimes a steep acceleration at the onset of firing (Fig. 1A ii and iii) (Bennett et al. 2001b; Hounsgaard et al.

1988; Lee et al. 2003; Li et al. 2004). Importantly, after the termination of the synaptic current that triggers the I_P (Fig. 1A v, dashed line), the extra depolarization from the I_P produces continued firing (self-sustained firing; Figs. 1A ii and iii), a phenomena that has been used extensively as an estimate of I_P in humans (Gorassini et al. 1998; Kiehn and Eken 1997). However, this self-sustained firing is only produced by *the portion of the* I_P that is activated after the firing onset (after the red and purple dashed lines in Fig. 1A iv), making it generally an underestimation of the I_P. In the extreme case when the I_P and plateau potential are fully activated by the synaptic input prior to the onset of firing (Fig. 1A i, pink), or when the I_P and firing are fully activated before the stretch-evoked synaptic input (Fig. 1A vii, blue), the I_P cannot further boost or prolong firing, with the firing rate profile proportional to the synaptic input profile (no self-sustained firing). Likewise, when there is a residual I_P activated by a prior activation of the motoneuron, the I_P does not further activate and the firing rate only increases gradually in proportion to the gradual increase in synaptic input with no self-sustained firing (Fig. 1A vi, black). Thus, the largest self-sustained firing seems to occur when the I_P and firing onsets are simultaneous, allowing maximal facilitation of firing by the I_P (Fig. 1A iii, red).

< Insert Figure 1 near here >

It is also possible to measure self-sustained firing produced by I_P from a symmetrical, triangular current injection into the motoneuron. When the I_P is activated by current injection into the soma of a motoneuron, there are three classically defined linear regions of the firing rate response: first if the I_P is not initially activated at all, there is sometimes a gradual increase in firing with current (primary range; Fig. 1B v, black line) (Heckmann et al. 2005; Li et al. 2004). However, this primary range is uncommon and now considered an artifact of injecting current into the soma near the sodium channels underlying the spike and far from the dendritic locations where most I_P and synaptic inputs occur (Bennett et al. 1998b; Lee and Heckman 2000). Thus, current injection into the soma favors spiking over I_P activation, whereas natural synaptic input does the opposite, activating the nearby I_P first before spikes as detailed above. Second, as the membrane potential is depolarized further, the firing rate abruptly increases more steeply as the I_P is

being activated (secondary range; Fig. 1B v, pink line); this is how many motoneurons start firing with current injection, at least briefly in the secondary range (Li et al. 2004). Finally, after the I_P is steadily activated the firing rate increases more slowly due to an increased conductance provided by the I_P and associated calcium activated K^+ currents (tertiary region, Fig. 1B v, green line) (Li and Bennett 2007). Some motoneurons start firing directly in the tertiary range (Fig. 1B i) (Li et al. 2007). Using this terminology for responses to natural synaptic activation of firing detailed above, firing is initiated either in the secondary range (Figs 1A ii and iii) or directly in the tertiary range (Figs. 1A i and vi) because the I_P is always activated subthreshold to firing (Bennett et al. 2001a; Gorassini et al. 1999; Kiehn and Eken 1997; Li et al. 2004), and primary range firing likely never occurs (Bennett et al. 1998b).

The self-sustained firing can be quantified systematically during these slow triangular somatic current injections, as follows: after an increasing current ramp activates an I_P and the cell is firing in its secondary or tertiary range, the current can be decreased with a similar slow, but descending current ramp, to ascertain how much the I_P contributes to sustain firing (Bennett et al. 2001a; Li et al. 2004). Usually, the firing rate continues in the tertiary range until near de-recruitment, and then sometimes drops steeply as the I_P is terminated and firing stops (Fig. 1B v, downward pink arrow to denote secondary range at de-recruitment). Importantly this firing on the descending current ramp continues at injected current levels below the current needed to initiate firing (compare blue dots in Figs. 1B i-iii), and only stops when the injected current is below the onset current by a value of ΔI that reflects the contribution of the I_P to self-sustained firing (height of boxes in Figs. 1B i-iii). Again, only *the portion of the* I_P activated after the onset of firing contributes to self-sustained firing (ΔI; tip of the I_P iceberg so to speak). Thus, motoneurons having firing thresholds that are closer to the I_P onset voltage yield the largest ΔI values (red, Fig. 1B iii), for a given fixed I_P size. Theoretically, if the I_P is fully activated entirely sub-threshold to firing, the motoneuron begins to fire directly on its tertiary range and responds proportionally to the injected current, starting and stopping firing at the same level of injected current to

yield no self-sustained firing ($\Delta I = 0$). In this case, the contribution of the I_P to the activation of the motoneuron cannot be reflected in its discharge behaviour because the effects on the membrane potential are all sub-threshold to firing.

Sometimes the I_P slowly decreases with time (sags) during these slow triangular current ramps and this can lead to a downward offset in firing rate and less self-sustained firing (Fig. 1B iv, grey line above green non-inactivating I_P). This sag could have a number of causes, including calcium and sodium I_P inactivation (Lee and Heckman 1999; Powers and Heckman 2017) or buildup of calcium-activated potassium (SK) currents (Li and Bennett 2007). The downward offset in firing rate can also be mediated by a rate (direction)-dependent effect of the depolarizing drive on spiking (Kuo et al. 2006; Norton et al. 2008). Faster current ramps should avoid this minor non-linearity (Revill and Fuglevand 2011), a topic we address latter in this paper.

When the I_P is fully activated (in the tertiary range), motoneurons often respond remarkably linearly to both increasing injected current or synaptic current, with the firing rate profile (Fig. 1A vi and vii) accurately reflecting the synaptic input profile (grey line, Fig. 1A v) (Bennett et al. 1998b; Lee et al. 2003). Using this linearity we previously developed a method of estimating the synaptic input to a motoneuron pool from the firing (F) of a continuously firing low threshold motor unit (control unit), assumed to be in its linear tertiary range (Bennett et al. 2001a; Gorassini et al. 2002a; Gorassini et al. 1998). This estimate of the synaptic input (F) was then used to compute the degree of self-sustained firing of higher threshold motor units (test units), exactly as we have described for current injection (ΔI calculation), but in this case having participants make triangular force contractions, rather than current injection, to produce a triangular synaptic input profile. Here we measure the difference in the synaptic input needed to terminate firing of the test unit (control unit firing, F_T) compared to the synaptic input needed to recruit firing (control unit firing, F_R), $\Delta F = F_R - F_T$, as a measure of the self-sustained firing produced by the I_P, but otherwise all the issues discussed above for ΔI remain the same. This method has

been verified by measuring ΔF in low threshold motor units in awake rats and then measuring ΔI and the F-I slope (S) with direct intracellular recordings from motoneurons in these same rats, yielding ΔF = S * ΔI (Bennett et al. 2001a). The ΔF and ΔI method has also been validated with computer simulations (Elbasiouny et al. 2006; Powers and Heckman 2015; Powers et al. 2008; Revill and Fuglevand 2011). Subsequently, the paired unit method has been extensively used in humans, but mostly restricted to low threshold motor units where we know the linearity assumption for the control unit firing holds [reviewed in (Binder et al. 2020; D'Amico et al. 2013; Heckman et al. 2008; Heckmann et al. 2005; Johnson et al. 2017)]. Importantly, this motor unit activity to estimate ΔF has mainly been obtained from intramuscular EMG where it is only possible to identify a few low-threshold test motor units during moderately strong contractions (~10% MVC or less). Thus, we know little about I_P activation in higher threshold test units, a topic we address in this paper.

With the advent of new high-density surface EMG arrays and advances in motor unit identification algorithms we now have the ability to non-invasively identify 20 or more motor units per muscle (such as the tibialis anterior) over a wide range of recruitment thresholds, potentially up to 100% MVC (Del Vecchio A 2020; Holobar and Farina 2014; Martinez-Valdes et al. 2016; Negro et al. 2016a). This provides the opportunity to estimate self-sustained firing from many more motoneurons and examine how this differs with motoneuron size. However, it also presents a serious computational problem when estimating ΔF, since there are typically over 20 possible control units to choose from that can each be paired with all other higher threshold test motor units to compute a ΔF (Hassan et al. 2019). So for a given test motor unit, which is the best control unit to pair it with, or should all possible pairings be admitted? Firing rate profiles of motor units during triangular force contractions can have varying degrees of linearity, with some motor units exhibiting very symmetrical linear firing rate profiles suggestive of tertiary range firing (as in Fig. 1B i, vi and vii), whereas other motor units exhibit an initial sharp increase in firing rates indicative of secondary range firing with I_P activation during recruitment

184 (as in Fig. 1A ii and iii) (Bennett et al. 2001a; Binder et al. 2020; Gorassini et al. 1999), likely making
185 them poor control units.

186 In this paper, we developed methods to determine how to best represent the synaptic input profile
187 from several control motor units that likely have the best linear input-output firing behaviour (i.e.,
188 tertiary range firing), an important requisite for the accuracy of ΔF measures in representing self-
189 sustained firing produced by I_P. The firing properties of simultaneously recorded tibialis anterior (TA)
190 motor units that were activated during a triangular 10-s up and 10-s down isometric contraction were
191 characterized. Voluntary contractions were performed at 10%, 20% and 30% of maximum (MVC)
192 where ≈ 70% of all motor units are estimated to be recruited at 30% MVC (Feiereisen et al. 1997). This
193 produced contractions with different speeds over the same time period (i.e., 1%, 2% and 3% MVC per
194 second), allowing us to also examine the effect of contraction speed on I_P. Firing properties of the TA
195 motor units (motoneurons) during various phases of the contraction and estimates of the contribution of
196 the I_P to self-sustained firing (ΔF values) were compared between motor units of different recruitment
197 thresholds, ultimately allowing us to examine our central questions of how the I_P varies in different size
198 motoneurons, and how suprathreshold I_P activation affects firing in motor units of different sizes.

199 Finally, one noted constraint in using the firing rate of a control motor unit to represent the synaptic
200 drive to a test unit is the extent to which its firing rate varies with synaptic input (i.e., firing rate
201 modulation). In both animals and humans, ΔF values measured in test units can be positively correlated
202 to the amount of firing rate modulation in the control motor unit, raising the issue that the amplitude of
203 the ΔF is constrained by how much the firing rate of the control motor unit can change in response to a
204 changing synaptic input (Powers et al. 2008; Stephenson and Maluf 2011). A possible source of reduced
205 firing rate modulation in a control unit is rate saturation where increases in synaptic current are not as
206 efficiently transduced into a proportional increase in the rate of action potential generation (Fuglevand et
207 al. 2015; Revill and Fuglevand 2011; 2017). Here, we examined if similar issues with rate saturation and

208 rate modulation constrained our measures of ΔF values at the different contraction strengths when using
209 motor units decomposed from high-density surface EMG. Lastly, we measured the proportion of time a
210 motor unit was firing in its I_P-mediated, self-sustained firing range and how this may change with
211 recruitment threshold of the motor unit.

METHODS

Experiments were approved by the Health Research Ethics Board of the University of Alberta (Protocols 00023530 and 00076790) and conformed to the *Declaration of Helsinki*. Ten neurologically intact participants (6 female, 4 male) aged 21 to 58 years took part in this study. All participants gave written informed consent prior to participation.

EMG recordings: Flexible, high-density surface EMG (HDsEMG) electrodes (GR08MM1305, OT Bioelecttronica, Inc., Turin, IT) were used to record from 64 sites on the tibialis anterior (TA) and soleus muscles of the dominant leg. The recording sites were arranged in a 5×13 grid with 8 mm inter-electrode distance in both the x and y direction. The 5 columns of electrodes were orientated in the x direction from lateral to medial and the 13 rows of electrodes were orientated in the y direction from proximal to distal. To maximize the signal-to-noise ratio, the skin was rubbed lightly with abrasive paste (NuPrep, Weaver and Company, Colorado USA) and any remaining residue was removed with saline (Hermens et al. 2000) to reduce impedance between the electrode and skin (Merletti 2016). Electrodes were placed over the entire TA and soleus muscle bellies whose boundaries were visualized from a voluntary contraction. The electrodes were secured to the skin using flexible tape (3M Transpore Clear Plastic Tape, London, Canada). All 64 EMG signals were recorded in a monopolar configuration, where the EMG potential recorded from one grid electrode was referenced to a strap electrode placed around the lower leg near the ipsilateral ankle or knee joint. A Quattrocento system (OT Bioelettronica, Inc., Turin, IT) was used to amplify the HDsEMG signals (x150) with filtering set to 10 Hz high pass and 900 Hz low pass, sampled at 5120 Hz, digitally converted (16-bit resolution) and then transferred to a PC. The duration of each file was kept below 200 s to be manageable for post-processing. Only data obtained from the TA muscle is reported here. The TA muscle was chosen because HDsEMG from the TA typically produces a larger number of decomposed motor units for contractions of 10 to 30% MVC (Del Vecchio A 2020).

Experimental task: Participants were seated comfortably with their foot resting on a custom 3-D printed holder coupled to a 150 lb S-type Load cell (Interface Force Measurement Solutions, Arizona) and with the knee and ankle angle at ~120° of extension and plantarflexion, respectively. A visual display of the exerted dorsiflexion torque was presented on a computer screen, and participants were instructed to track a triangular line drawn on a transparency overlaid on the display. The horizontal (y) scale of the computer display was adjusted to modify the strength of the contraction expressed as a percentage of the participant's maximum voluntary contraction (% MVC) obtained by averaging the maximum torque produced from two maximal contractions. At least 6-10 contractions were measured at 10%, 20% and 30% of MVC over 2 to 3 trials. The 6 trials with the smoothest and most symmetrical torque profiles were chosen for analysis (see example good trial in Fig. 2). Within a trial, each contraction was separated by at least 20 s to avoid frequency-dependent facilitation of the motor units (Gorassini et al. 2002b; Hornby et al. 2003). Contraction duration was set to 10 s for both the ascending and descending phase of the triangular contraction, producing rates of contraction/relaxation of 1%, 2% and 3% MVC/s for the 10%, 20% and 30% MVC contractions, respectively.

< *Insert Figure 2 near here* >

Data analysis:

Single motor unit identification: Once the data were recorded and stored on a local computer, the files were then converted into a Matlab file format. MATLAB ver. R2018b/ R2019a and custom built functions were used for data processing and analysis. Before the decomposition process, the sEMG data were divided so that only one contraction was included in a single data file in order to decrease computation time. Further pre-processing included offset removal, band-pass filtering (4th order, Butterworth, zero lag, digital-filter, 10-500 Hz), and power line interference attenuation using a notch filter. We performed visual inspection of all HDsEMG signals to identify bad channels displaying

substantial noise or artifacts. If there were more than 6 bad channels (≈10% of the 64 channels in the grid) the data were not used.

The remainder of the HDsEMG signals were decomposed into motor unit spike trains (referred to as pulse trains) using the validated decomposition method of convoluted blind source separation (Martinez-Valdes et al. 2017; Negro et al. 2016a). The threshold for the value used to assess the reliability of the estimated discharge timings, or the silhouette value (SIL) (Holobar et al. 2014), was set to 0.85 (Negro et al. 2016a). For a given motor unit that was isolated from the other units, the decomposition algorithm estimated the time of firing for that unit (termed pulse, bottom trace Fig. 2A) and the inverse of the interval between pulses was displayed as instantaneous firing rates (third trace, Fig. 2A). The amplitude of the pulse was interpreted as the confidence (accuracy) of the algorithm to assign the motor unit to that instant of time relative to nearby pulses buried inside the noise within the pulse train. Thus, the amplitude of the pulse is in arbitrary units and can be interpreted as an indication of the pulse-to-noise ratio. However, some of the pulse amplitudes were slightly above the noise level (e.g., above 4-6 a.u. in Fig. 2A bottom trace) but below the level of nearby pulses that were selected by the k-means clustering used in the algorithm (selected pulses marked by red circles, missed pulses marked with black circles). Because these missed pulses produced firing rates that were half of the mean rate (small black arrows, third trace), and likely not physiological, we manually and iteratively included them and re-estimated the pulse train (dashed blue arrows in bottom trace point to the re-estimated pulse marked by the dotted red circles) to correct the frequency profile (second trace, Fig. 2A) as per (Boccia et al. 2019; Del Vecchio A 2020; Hassan et al. 2019; Martinez-Valdes et al. 2020). In other cases (not shown), the algorithm incorrectly assigned 2 or 3 pulses to what was likely only a single pulse (i.e., a single discharge time), resulting in instantaneous firing rate(s) that were well above the mean rate. Here, the extraneous pulse(s) were also manually removed and the final pulse trains were re-estimated. The majority of estimated pulse trains (≈ 90%) required manual editing and once the decomposition accuracy was recalculated after the edit, the accuracy (silhouette) value either increased or only decreased slightly by <0.01.

286 Data from three subjects were excluded from further analysis because the average number of
287 decomposed motor units per contraction was less than 7. The excluded participants were 8F (female
288 aged 42: 6.5 ± 1.5 units, range 3-8, median 7 units), 9F (female aged 26: 5.5 ± 1.2 units, range 3-7,
289 median 5 units) and 10F (female aged 21: 1.9 ± 1.8, range 0-6, median 1 unit). In these participants there
290 were not enough low threshold control motor units to obtain ΔF measures for the required 6
291 contractions.
292
293 *Parameters measured from the raw firing frequency profile:*
294 *Number of units, accuracy and threshold.* The number of units isolated per contraction and the accuracy
295 value of the decomposition for each unit (SIL) were measured and averaged across the 6 trials for each
296 of the 10%, 20% and 30% MVC contraction levels (Figs. 2B and C; values for each participant are listed
297 in Supplemental Table 1). As with all measurements, the mean value for each of the 7 participants was
298 averaged across the group, and along with the standard deviation values, presented at the bottom of the
299 Supplemental Tables and in the figures. Supplemental Tables are located in the Figshare data
300 repository: https://doi.org/10.6084/m9.figshare.12067344. To establish the recruitment order of the
301 multiple decomposed motor units in a given contraction, the level of torque when a motor unit was
302 recruited was measured (Fig. 2A, top trace) and expressed as a % of MVC.
303 *Parameters measured from the polynomial line fit to the firing frequency profile:* The firing
304 frequency profiles for the decomposed motor units were estimated by fitting a 5^{th} order polynomial line
305 to the instantaneous firing frequency values (green line, Fig. 2A third trace). The coefficient of
306 determination (r^2) of the fit line was averaged for all units at each contraction strength in each participant
307 and this mean was then averaged across all participants (R^2 Polynomial, Fig. 2D). The start, maximum
308 and end firing rates were measured from the polynomial line for all units in addition to the firing rate of
309 the control motor units during recruitment and de-recruitment of the test motor units. To determine the
310 maximum change in firing rate of a control unit during the contraction, the difference between the

maximum and minimum firing frequency from the polynomial line, termed the modulation depth (MoD, third trace), was measured (Fig. 2A, third trace).

Although the polynomial line provided a relatively accurate measure of the control unit firing rate when the test unit was recruited and de-recruited, the peak of the polynomial line was shifted slightly to the left of the peak torque as demonstrated when fitting a straight line to the secondary (pink) and tertiary (green) firing range (Fig. 2A, second trace). Note that the firing rate during the ascending tertiary range increases until peak torque. As the torque began to decrease during the descending phase of the contraction, the firing rate dropped to a lower offset (sag) and continued to decrease at a similar rate (slope) as on the ascending phase [see also (Bennett et al. 2001a; Gorassini et al. 1999; Powers and Heckman 2017)]. This is in contrast to the profile of the fit polynomial line (green, third trace) where the peak occurs ≈ 1.5 seconds earlier. Upon visual inspection, all firing rate profiles peaked at maximum torque and then began to sag at the onset of the torque decline during the descending phase of the contraction. Thus, we used the peak of contraction torque, rather than the peak of the polynomial line, to indicate the transition point from an ascending to a descending synaptic input which was important for the measurement of self-sustained firing duration described below. Lastly, to obtain an overall value of the rate of increase or decrease in firing rate of a motor unit, the slope of the straight line fit to the ascending or descending phase of the polynomial line (Asc Slope and Desc Slope, marked by pink dashed line in Fig. 2A, third trace) was measured. For each contraction level, all measures were averaged across the 6 trials in each participant with the mean ± standard deviation presented in Supplemental Table 1 along with the average of these means (total) across the 7 participants.

ΔF measurement: Estimation of the I_P contributing to self-sustained firing was estimated from pairs of motor units as described previously where the lower threshold "control" motor unit of the pair was used as an estimate of synaptic input to a higher threshold "test" motor unit of the pair (Gorassini et al. 2002a). The firing rate of the control motor unit (values taken from the fit polynomial line) when the test

motor unit was de-recruited was subtracted from the control unit rate when the test motor unit was recruited to obtain a ΔF value. All possible combinations of relatively lower and higher threshold motor unit pairs were used to measure ΔF for a given contraction and we referred to this as "pairwise ΔF". As described in more detail in the Results, we also constructed a composite control motor unit profile where the firing frequency profiles of the lowest threshold motor units were plotted together and a new 5th order polynomial curve was fit to the combined data. The selection criteria for a composite control motor unit were a recruitment threshold of less than 3% MVC with a secondary range of less than 2 seconds. Of the total number of decomposed motor units in each contraction (≈ 20), there were typically 3 to 6 of them with recruitment thresholds less than 3% MVC. In these units the steep secondary range, as identified visually, was around 1.5 s (detailed in Results), so the majority of firing occurred in the linear tertiary range. In 4 of the participants, typically one low threshold control motor unit in half of the contraction trials had a very shallow tertiary slope and low (< 5 Hz) firing rate modulation (0.4 ± 0.8 units per contraction). These units were not used as controls and removed from the dataset. The remaining units that were recruited after the composite control units were then used as test units to measure the "composite ΔF".

In addition to the ΔF values, the coefficient of determination (r^2) of the relationship between the firing rate of the control motor unit and the firing rate of the test motor unit (i.e., rate-rate plots of control and test polynomial lines) was measured to determine if the control and test units were receiving a common synaptic input (Gorassini et al. 2002a). As with all other measures, this was done for the ΔF values using the pairwise and composite control motor unit methods (rate-rate r^2 values, Supplemental Table 3). The interval of time between the recruitment of the control and test motor unit was also measured (ΔT recruitment) and plotted against the corresponding ΔF value to determine if this affected ΔF (Hassan et al. 2019; Udina et al. 2010).

Self-sustained firing duration: To obtain a measure of the proportion of the total time the test unit was firing at synaptic inputs below the level required to recruit the motor unit, we measured an index of the self-sustained firing duration (SSD). That is, if there were no I_P activation, the motor unit would stop firing at the same level of synaptic input that was needed to initially recruit the unit (at dashed grey vertical line in Fig. 1A). Activation of the I_P after recruitment allows the motoneuron to fire for longer below this level of synaptic input to produce self-sustained firing (pink shaded area in Fig. 1Aii and iii). We calculated the SSD as follows (further detailed in Fig. 10):

$$\frac{\text{(time of firing during descending phase - time of firing during ascending phase)}}{\text{(time of firing during ascending phase + time of firing during descending phase)}} \times 100\%$$

As described above, we used the peak of the contraction torque to indicate the transition point from an ascending to a descending synaptic input from which we measured the time of motor unit firing during the descending and ascending phase of the contraction.

Statistics: Example data is presented for each of the 7 participants in the various figures. Data are described in the figures and supplemental tables as means and standard deviations for both individual participants and the average of the means across the 7 participants. Sigma Plot 11.0 software was used for all statistics. Across the group, Mann-Whitney Rank Sum Tests were used to compare various parameters of the firing frequency profiles such as start vs. end rates, ascending vs. descending slopes and pairwise ΔF vs. composite ΔF values. A Bonferroni correction to a significance level of $P < 0.025$ was used to account for the multiple comparisons at the 10%, 20% and 30% MVC contractions. Pearson's product moment correlation (r) was used to determine if there was an association between ΔF and control unit modulation depth (CMod). The coefficient of determination (r^2) was calculated for the polynomial line fit to the frequency profiles and to the linear line fit to the control rate-test rate plots, as described previously (Gorassini et al. 2002a). A one-way, repeated measures ANOVA was used to

385 determine if ΔF, ascending slopes and SSD varied with recruitment threshold of the test unit.
386 Appropriate post-hoc t-tests were used to determine if values for the lowest threshold test units were
387 different from the higher threshold units.
388

RESULTS

Motor unit decomposition from HD-sEMG

For a given isometric contraction, a maximum of 6 to 40 single motor units were identified from the decomposition of the 64 channels of monopolar HD-sEMG in the ten participants tested. Data from three participants (all female) were not included because less than 8 motor units were identified per contraction (details in Methods), with too few low threshold control units to obtain ΔF values for the required 6 contractions. In the remaining seven participants, an average of approximately 20 TA motor units were decomposed per contraction at the 10%, 20% or 30% MVC isometric contractions (Fig. 2B, see Suppl. Table 1 for individual participant values). Accuracy or silhouette values (described in Methods) in decomposing the single motor units was 0.95 (95%) on average for all participants (Fig. 2C, Suppl. Table 1), with firing rate profiles well fit by a 5^{th} order polynomial as reflected in an average coefficient of determination (r^2) between 0.73 and 0.76 for all contraction levels (Fig. 2D, Suppl. Table 1). All Supplemental Tables are located in: https://doi.org/10.6084/m9.figshare.12067344.

Firing rate profiles of decomposed motor units

When participants produced slowly increasing and then decreasing triangular isometric contractions (10s up and 10s down), the decomposed motor units were gradually activated in order of their recruitment threshold (Fig. 3A, motor units displayed in ascending order of recruitment threshold). Once recruited, the firing rate of the motor units typically increased linearly over most of the ascending ramp until peak torque was reached (at gray dashed line). Immediately following the downward turn in torque during the decreasing effort, the firing rate decreased, again linearly with a slope similar to the ascending phase. However, the slope of the straight line fit to the descending phase was shifted slightly downward (marked in Unit 1 by lower green line), likely due to sag as detailed in the Discussion. These similar upward and downward linear slopes indicate that the firing rates increased and decreased without much rate-saturation during the 10 s of increasing and decreasing effort (see also Fig. 2A in Methods).

We thus considered the peak torque to indicate the peak of the synaptic drive. When a 5th-order polynomial line was fit to the firing rate profile of each unit, the peak of this smooth line was slightly before the peak torque, likely because of the smoothing and the sag mentioned above. However, this polynomial line still provided a relatively accurate representation of the rate of increase and decrease of the firing rate profile (see r^2 values, Fig. 2D), and importantly, the firing rate at recruitment and de-recruitment of the test motor units.

In many units the firing rate started with a high initial firing rate and a steep increase in rate (secondary range, pink), likely due to the I_P onset; following this the firing rate then increased more slowly with a more shallow slope (in tertiary range, green line: e.g., Unit 10, Fig. 2A). Upon decreasing the force, the firing rate decreased with a similar shallow slope (tertiary range). Because of the larger secondary range at the onset of firing, the slope of a line fit to the entire ascending phase of the firing rate profile was, on average, steeper compared to the descending phase slope (Figs. 4A i and ii, Suppl. Table 1), consistent with I_P activation at the onset of recruitment, which accelerates initial firing rates. Likewise, the average rate at the start of the firing profile was higher compared to at the end of firing (de-recruitment) (Fig. 4B), consistent with activation of the I_P at recruitment.

< Insert Figures 3 and 4 near here >

A common feature across all contraction levels was that the slope of the ascending firing rate profile increased as the recruitment threshold of the units increased (Fig. 4C), as also illustrated when plotting all polynomial lines from Figure 3A together (Fig. 3B). The shallow slopes of the lowest threshold units (e.g., Units 1-3 in Fig. 3A) likely represent motoneurons where the majority of the I_P was recruited below the firing threshold and thus, with the majority of firing occurring in the tertiary range (green lines in Unit 1). In higher threshold units (4-19) there were more pronounced and prolonged steep increases in firing at recruitment, producing a prolonged secondary range, likely resulting from I_P activation at recruitment (e.g., pink line in Unit 10). The slope shallowed during the tertiary range after

full I_P activation (green lines in Unit 10), but this tertiary range firing was of shorter duration, and so the overall ascending slope was often dominated by the secondary range in these higher threshold units.

Estimation of I_P-mediated self-sustained firing from individual motor unit pairs (pairwise method)

The firing rate profiles from the multiple decomposed motor units were used to estimate the self-sustained firing produced by I_P (ΔI) from the paired motor unit analysis (ΔF). As described in the Introduction, the amount of depolarization provided by the I_P to maintain firing of a test motoneuron can be estimated from the difference in synaptic input needed to maintain minimal firing after the I_P is fully activated (measured at firing termination, F_T) compared with the larger synaptic input required to initiate firing *prior* to full I_P activation (measured at recruitment, F_R). Here, synaptic input to a test unit is estimated by the firing rate profile of a relatively lower threshold control motor unit. Thus, the self-sustained firing produced by I_P can be estimated as $\Delta F = F_R - F_T$. As illustrated in Figure 3C (left graph), a low threshold control motor unit (Unit 1 from Fig. 3A) was used as an estimate of synaptic input to a relatively higher threshold test motor unit (Unit 2). The firing rate of control Unit 1 when test Unit 2 was de-recruited (6.2 Hz) was subtracted from the firing rate of control Unit 1when test Unit 2 was recruited (7.3 Hz) to produce a ΔF value of 1.1 Hz for test Unit 2. Many permutations of control and test units are possible, and we systematically computed them all. Specifically, all higher threshold units (2 -19) were paired with control Unit 1 to compute a ΔF value. Following this, Unit 2 was used as a control rather than test motor unit, and ΔF values were computed for Units 3 to 19 and so on. All ΔF values for the 171 possible test-control unit pairs [(19x18)/2] are plotted in Fig. 3E according to the recruitment threshold of the test unit, with each test unit colour coded as in Figure 3A. Note the number of ΔF values increased by one as the recruitment threshold of the test unit increased because it was paired with an additional control motor unit.

There are two basic ways to consider the pairing of control and test motor units. First we can examine the ΔF values of different test units when paired with a common control unit. For example, when using the lowest threshold unit as a control unit (Unit 1) and measuring the ΔF in the next lowest threshold test unit (Unit 2), and then a much higher threshold test unit (Unit 9 recruited at 11% MVC), ΔF values of 1.1 Hz and 3.7 Hz are produced, respectively (Fig. 3C). On face value this suggests that the lower threshold Unit 2 had a smaller I_P contributing to self-sustained firing. However, as we detail below (see floor effect), this lower ΔF could be because Unit 2 was activated when control Unit 1 fired at a very low rate, perhaps underestimating the ΔF value.

The other way to pair units is to compute the ΔF for a single test unit with different control units. For example, pairing test Unit 17 with control Units 13 and 6 lead to very different ΔF values of -0.3 Hz and 5.2 Hz, respectively (Fig. 3D). More generally, when all possible pairings of different control units to a given test unit were made, there are a large number of possible ΔF values computed, even though a given test motoneuron can only have one I_P value. This is particularly concerning since we find that the ΔF for a given test unit varied by as much as 8 Hz depending on the control unit it was paired with (Fig. 3E) [see also (Hassan et al. 2019)]. This variability is largely due to variations in the firing linearity of the control unit and the timing of its onset relative to the test unit. Thus, in the next few sections we detail methods to identify and eliminate inappropriate pairings of control and test motor units.

a) Floor effect and early control unit de-recruitment errors:

When a low threshold test unit (Unit 2) was recruited shortly after its even lower threshold control unit started firing (Unit 1), the control unit typically fired at a very low rate (Fig 3C left). Thus, this estimate of synaptic input (Unit 1 firing rate) had little room to be reduced at de-recruitment of the test unit, since the firing rate of the control unit cannot go much lower (floor effect). This floor effect contributed, in part, to the artificially low ΔF values for the lowest threshold motoneurons (detailed more

in Fig. 9). In other cases (such as comparing control Unit 14 to test Unit 15, Fig. 3A), the control unit stopped firing prior to the test unit, making the estimate of synaptic input at de-recruitment higher than it should be (or unknown) to artificially underestimate the ΔF value.

b) Nonlinear firing of control unit during I_P activation leads to underestimation errors.

As mentioned above, only the lowest threshold units that fire predominantly in the tertiary range following full or nearly full I_P activation likely provide the most accurate and linear representation of the synaptic drive, like Unit 1 in Figure 3C. Higher threshold units that often have non-linear firing due to a prolonged secondary range that transitions to a tertiary range many seconds after recruitment provide less accurate measures of synaptic input and thus, should not be used as control units. For example, when Unit 13 with a steep secondary range at the onset of firing was used as a control unit, it produced a very low ΔF value when paired with test Unit 17 (Fig. 3D, left graph). This is because at the time test Unit 17 was recruited, the I_P in Unit 13 was likely not fully activated and its firing rate underestimated the synaptic drive at this time, relative to the estimate at de-recruitment when the I_P was fully activated, ultimately giving a low ΔF (-0.3 Hz).

To further illustrate this error in underestimating the ΔF, the ΔF values for each of the 6 contraction trials at 10%, 20% and 30% MVC were plotted for all motor unit pair combinations measured from the 19 units in Figure 3A (Fig. 5A). These pairwise ΔF values were plotted against the time difference between when the control unit was recruited and the time when the test unit was recruited (ΔT recruitment). In general, this revealed an underestimation and wide variability of the ΔF at short test-control ΔT recruitment times between 0 and 2 s (as for test U17 vs control U13, Fig. 3D). The ΔF values then leveled off when the test units were recruited at least 2 seconds after the control unit, because the test units were no longer being recruited while the control units were within their initial, low-frequency secondary range (as for test U9 vs control U1, Fig. 3C). This leveling effect occurred for

all ramp speeds (1-3% MVC/s) at the 3 different contraction strengths (Fig. 5A), although the large variability in ΔF values continued past ΔT times > 2s. The mean ΔF for the multiple pairwise comparisons was similar across the 10%, 20% and 30% MVC contractions (p all > 0.59, black bars: Fig. 5D, Suppl. Table 2).

< Insert Figure 5 near here >

c) Nonlinear firing of control unit during I_P deactivation leads to overestimation errors

A control motor unit could also have an early, steep deceleration in firing rate when a test unit is de-recruited, as often occurred with the high threshold units (e.g., Units 17 and 18 in Fig. 3A). Here, the amount of synaptic input would be underestimated during test unit de-recruitment which would also produce an overly large ΔF value. Because the slope of the descending phase of the firing rate profiles increased with recruitment threshold of the units (Fig. 4D, see also polynomial overlays in Figure 3B), this produced varying estimates of synaptic input in different control units for a single de-recruitment time of a given test unit. Thus, the variable times that the I_P was deactivated to produce the different slopes of descending firing rate contributed to the variability in ΔF values for a single test motor unit, especially for the higher threshold test units.

d) Variation in control unit sensitivity to synaptic input errors

Higher threshold units had, on average, higher slopes in their firing rate both on the ascending and descending phases of the ramp (Figs. 4C and D), and could reach higher firing rates compared to the lower threshold units (see polynomial overlays from participants 1F and 5M, Fig. 3B). This made the higher threshold units more sensitive to changes in synaptic input and thus yielded higher ΔF values when these units were used as control units, compared to the low threshold control units. Thus, it is

advisable to settle on a single, low threshold control unit (or collection of low threshold units) to measure ΔF values in all the other test units as we detail next.

Measurement of ΔF from a composite control motor unit profile

In order to reduce the number of underestimated and overestimated ΔF values (detailed above), we developed a new method where only the lowest threshold control units that fired primarily within their linear tertiary range were used as estimates of synaptic input to the test units. For each contraction, we selected the lowest threshold motor units (< 3% MVC, typically 3-6 units) to construct a *composite* control unit profile (Fig. 6). Compared to the higher threshold units, the lowest threshold units had the shortest initial firing rate accelerations (secondary range) and proportionally longer periods of tertiary range firing. We assumed that in these low threshold units, the I_P was almost fully activated at the time of recruitment so that their firing rate profiles were more linearly related to the synaptic input profile. An example is shown in Figure 6A where the firing rates of the 3 lowest threshold units from Figure 3A (Units 1 to 3) are superimposed to form a "composite" control motor unit profile. In these units there is a brief, initial acceleration in firing rate (secondary range, pink line) and afterwards, the firing rate increases less steeply during the tertiary range (green line). To restrict the composite control unit profile to a single linear range, the firing rate values within the secondary range were identified visually and removed. A new polynomial line (red) was then fit to the edited profile (Fig. 6B). Because of the short duration, the secondary range in these low threshold control units was easy to distinguish visually from the tertiary range. On average, the first 1.1 ± 0.3 s of the firing rate profile was removed for the 10% MVC contractions, 1.5 ± 0.4 s for the 20% MVC and 1.5 ± 0.3 s for the 30% MVC contractions, with the start of the edited composite control profile occurring before any higher threshold test unit was recruited. Following removal of the secondary range firing, the ascending slope of the remaining composite control profile (i.e., tertiary range) was 0.63 ± 0.26 Hz/s for the 10%, 0.79 ± 0.26 Hz/s for the

20% and 0.90 ± 0.33 Hz/s for a the 30% MVC contractions, being lower than the average overall ascending slope of the higher threshold test motor units that had a proportionally longer duration secondary range firing (further described in Fig. 9B).

Removing the secondary range made the slope of the polynomial line on the ascending phase of the composite control profile similar to the descending phase, with an ascending/descending slope ratio near 1 (Fig. 6E, Suppl. Table 2), especially for the 20% and 30% MVC contractions. A matched ascending and descending rate of synaptic input is important when measuring I_P amplitude to avoid any rate-dependent effects on motor unit recruitment or de-recruitment (Desmedt and Godaux 1977; Freund 1983; Kuo et al. 2006). On average, around 4-5 of the lowest threshold motor units were used to construct the composite control unit profiles at each of the different contraction strengths (Fig. 6G, Suppl. Table 3). The downside of this method is that it does not allow us to estimate the ΔF of the lowest threshold units since they are used in the composite control profile. However, as discussed above these units have ΔF values that may be affected by floor effects from their even lower threshold control units and predominant sub-threshold I_P activation. Thus, these units should be viewed with caution.

< Insert Figure 6 near here >

The composite control profile reduced the variability of the ΔF values. For example, a ΔF value of 3.6 Hz was obtained when test Unit 17 from Figure 3D was paired with the composite control (Comp) profile (Fig. 6C). This was likely a more accurate estimate of I_P-mediated self-sustained firing compared to the ΔF values of -0.3 Hz and 5.2 Hz obtained with control units U13 and U6 having large secondary range firing. When all the ΔF values measured with the composite control method for this participant were compared to the ΔF values from the pairwise method (Fig. 5B), it is apparent that the very low and high ΔF values were eliminated by the composite control method, and that ΔF remained fairly constant regardless of when the test unit was activated in relation to the start of the composite control unit profile

581 (ΔT recruitment). The removal of some of the low ΔF values are simply because the short test-control
582 unit intervals could not occur. The decreased spread of ΔF values is clearly illustrated in Figure 5C for
583 the three contraction levels for this participant when using the composite control (Comp) method
584 compared to the pairwise (Pair) method. Likewise, the coefficient of variation (CoV: SD/mean) of the
585 ΔF values across all participants was reduced nearly by half when using the composite control method as
586 a result of removing the extreme, and likely inaccurate, ΔF values from some of the pairwise
587 comparisons (Fig. 5E, p all < 0.001, compare black and red bars). The CoV was reduced even though
588 the average number of total unit pairs from the 6 contractions at the 10%, 20% and 30% MVC trials was
589 ≈14 times less (Fig. 6H, Suppl. Table 2), with around 230 ΔF values per contraction in the pairwise
590 method compared to 16 ΔF values for the composite method. Despite a reduction in variability, the
591 composite control unit method did not change the mean ΔF across the group (Fig. 5D, p all > 0.65),
592 likely because an equal number of low and high ΔF values were removed. The average coefficient of
593 determination (r^2) of the control rate vs test rate plots (rate-rate; see Methods) was well above > 0.5 for
594 both the pairwise and composite control method (Fig. 6F, Suppl. Table 3).
595
596 *Constraints of modulation depth of control motor units on the ΔF*
597 If the firing rate of a control motor unit does not represent the full excursion of change in
598 synaptic input to the test unit, which may occur with rate saturation or weak synaptic drive, then the ΔF
599 value for a given test unit may be underestimated. As an indication of this, we plotted the maximum
600 firing rate excursion of a control motor unit (i.e., maximum rate - minimum rate = modulation depth or
601 CMod, Fig. 2 Methods) against the ΔF of the corresponding test unit to determine if ΔF was constrained
602 by the modulation depth of the control unit. When using the *pairwise* method, some of the ΔF values
603 rested on or near the line of unity (Fig. 7Ai, participant 5M), especially for the 10% MVC contractions
604 where the CMod of the control units was the lowest. Some of the points along the unity line indicate that

the ΔF values were likely constrained by the amount of rate modulation of the control motor unit, especially for test units with low ΔFs. The test units with large (and likely over-estimated) ΔF values on the line of unity were paired with high threshold control units having large, non-linear firing rate modulation. Although data points tended to move away from the unity line at stronger contractions, there was a significant positive slope when fitting a straight line between ΔF and CMod at all contraction strengths for the pairwise data (black bars in Fig. 7E; slope > 0, p all <0.001, Suppl. Table 2).

< *Insert Figure 7 near here* >

A similar trend was shown for the ΔF values obtained from the composite control unit profiles where the ΔF values moved further to the right of the unity line for the stronger contractions (Fig 7Aii) because ΔF remained fairly constant (red bars in Fig. 7D, Suppl. Table 2) while the modulation depth of the composite control profile (black bars) progressively increased as would be expected for increasingly larger synaptic inputs. In addition, the large ΔF values on the line of unity having high threshold control units were also removed in the composite control method. In this participant, the slope of the straight line fit to the ΔF and CMod data was close to 0 for the 20% and 30% MVC contractions, indicating no relationship between ΔF and CMod. Across the group, the ΔF - CMod slope was not different from 0 at the 20% and 30% MVC contractions (red bars in Fig. 7E, p all > 0.2, Suppl. Table 2), indicating that a lack of modulation of the composite control profiles were not constraining the ΔF measures at these higher levels of contraction, unlike that for the weaker 10% MVC contraction and for all of the pairwise ΔF values.

The maximum firing rate of the composite control unit profile ($CMax_{comp}$) also increased with contraction strength (Fig. 7B for participant 5M and Fig. 7D for group values). In some participants, the increase in maximal firing rate leveled off from 20% to 30% MVC (Suppl. Table 2). This may indicate some rate saturation of the control units at 30% MVC so that some of the ΔF values may have been

underestimated. Despite this, the test motor units were recruited at firing rates of the composite control profile (C_{RT}) that were smaller than the maximum composite control rates where rate saturation was less likely (Fig. 7C for participant 5M and Fig. 7D for group values, Suppl. Table 2].

ΔF of test units with short ascending activation (SA) time

A single composite control unit profile made it easier to examine the relationship between the recruitment threshold of a test motor unit and its ΔF value because the recruitment time of the composite control profile was anchored to a single value. In general, we found that the ΔF values did not change in motor units of differing sizes based on their recruitment threshold. However, as shown for the 30% MVC contraction trials in participant 6M (Fig. 8B), a population of test motor units that were recruited near the end of the ascending phase of the contraction (at 23% MVC or greater, red circles) had very low ΔF values. It is possible that these higher threshold units had a smaller I_P, as suggested from cat studies (Lee and Heckman 1998a; b; 1999). However, test motor units that were also recruited near the end of the 20% and 10% MVC contraction trials also had lower ΔF values (red circles in Figs. 8C and D), even though these units were recruited near 15% and 10% MVC, respectively. Critically, the same group of motor units that had low ΔF values at the top of the 20 and 10% MVC contractions (red) had higher, near normal ΔF values when examined during larger ramps (at arrows on the 30% MVC contractions, Fig. 8B). Thus, the low ΔF values are an artifact of being at the top of the contraction ramp, likely due to the amount of time the unit is active for during the ascending phase of the contraction as we detail next.

The dependence of activation time during the ascending phase of the contraction on the ΔF value is illustrated in Figures 8Ai-iii for 3 different test units from the 30% MVC data in Figure 8B. It is apparent that the test unit with a large ΔF that was recruited before 20% MVC fired for more than 2 seconds during the ascending phase of the contraction (Fig. 8Ai). In contrast, the test motor units recruited after 20% MVC that were activated for less than 2 seconds during the ascending phase had

lower ΔF values (Figs. 8Aii and iii). As shown previously, test motor units that fire less than 2 seconds during the ascending phase of the contraction will often have low ΔF and ΔI values (Li et al. 2007; Li et al. 2004; Stephenson and Maluf 2011; Udina et al. 2010). This may result from the I_P not being fully activated before the synaptic input begins to decrease and so when synaptic input is reduced during the relaxation phase of the contraction, the I_P is inactivated early. In fact, the ΔF values marked with red circles in Figures 8 B-D were all activated for less than 2 seconds on the ascending phase of the contraction and had ΔF values below the -1 standard deviation of the mean. There were other test units with short ascending activation times but whose ΔF values were closer to the mean (grey circles above the red circles). It is likely that the I_P in these units were sustained for longer periods of time despite a relatively shorter ascending activation time [see also Fig. 1 in (Li et al. 2004)]. Given the potential for motor units with short ascending activation (SA) times to not have full I_P activation, these units should be treated as a separate population. When removing these test units with short activation times from the data set (≈ 1-3 per contraction trial with < 2s of activation on the ascending ramp and ΔF < -1 SD), the CoV of the ΔF values was further reduced for the 20 and 30% MVC contractions ($p < 0.003$, Fig. 5E), but the average ΔF (Fig. 5D) and r^2 values for the rate-rate plots (Fig. 6F) remained the same (see Suppl. Table 3 for individual participant values). Thus, in all subsequent analysis we removed these test units with short activation times.

< Insert Figure 8 near here >

ΔF and motor unit recruitment threshold (motoneuron size)

Correcting for inappropriate control and test unit pairings with the composite control method (and more generally abandoning the pairwise method of using all possible unit pairings as outlined above), allowed us to more accurately compare the ΔF values for test motoneurons of varying sizes (recruitment thresholds), especially for the 20% and 30% MVC contractions where the ΔF was not

677 constrained by the control unit modulation depth. In the composite control method (green circles, Fig.
678 9A) the ΔF was found to be generally invariant across all motor units, with no effect of recruitment
679 threshold on the ΔF values for both the 20% and 30% MVC trials [$F(6,8) = 1.3$, $p=0.26$; $F(6,13) = 1.5$, p
680 $= 0.13$, respectively, One-way repeated measures ANOVA]. However, there was an overall effect of
681 recruitment torque on ΔF values for the 10% MVC trials ($F(6,4) = 3.1$, $p = 0.04$) but no ΔF value at a
682 given recruitment threshold was different from the others in post-hoc comparisons. In contrast for the
683 pairwise method (black circles, Fig. 9A), there was an effect of recruitment threshold on ΔF values for
684 all contraction levels and speeds at 10% [$F(6,4) = 3.1$, $p = 0.01$], 20% [$F(6,9) = 3.1$, $p < 0.001$] and 30%
685 [$F(6,14) = 3.1$, $p < 0.001$] of MVC, though we now consider this to be an artifact of errors we discussed
686 above arising from this method. Here, ΔF values with test units having the lowest recruitment thresholds
687 (0-2% MVC, arrowhead) were significantly smaller than many of the ΔF values having test units with
688 higher recruitment thresholds (marked by stars in Fig. 9B). In summary, the ΔF values measured from
689 the composite control method remained constant for test motor units of increasing recruitment threshold,
690 whereas the pairwise method leads to different, though incorrect conclusions. An invariant ΔF with
691 increasing recruitment threshold occurred even though the amount of secondary range firing of the test
692 units also increased with recruitment threshold, as reflected in the increasing slope of their ascending
693 firing rate profiles (Fig. 9B). The significance of this is explained in the Discussion.

694 *< Insert Figure 9 near here >*

695 *Self-sustained firing duration (SSD)*

696 The ΔF value provides a measure of how much the firing rate modulation of a motoneuron is
697 mediated by self-sustained firing from the I_P (amplitude estimate of self-sustained firing). For example,
698 the entire firing rate modulation of a motor unit, as measured from the composite control profile, was 6.8
699 Hz, 8.8 Hz and 10.5 Hz for the 10%, 20% and 30% MVC contractions, respectively. Given that the
700 average composite ΔF was 4.1 Hz, 4.5 Hz and 4.6 Hz at these contraction levels, we can estimate that

60%, 51% and 44% of the firing rate modulation of a motoneuron was contributed to by the I_P for the 10%, 20% and 30% MVC contractions respectively (although values for the 10% MVC should be used with caution). In addition to this *amplitude* estimate of self-sustained firing, we also determined how the I_P influenced the *duration* of the self-sustained firing, by measuring the proportion of firing time that continued at synaptic inputs below the level required to recruit the motor unit (see Methods for calculation). To do this a self-sustained firing duration (SSD) index was computed by subtracting the period of time the test unit was active during the ascending phase of the contraction ("a" in Fig. 10A) from the duration of time the test unit was active on the descending phase ("d" in Fig. 10A) and normalizing it by the total firing time of the test unit ("a + d" in Fig. 10A) to give: SSD = (d-a)/(a+d) * 100%. The SSD for the two example test units in Figure 10A i and ii are 50% and 14%, with ΔF values of 5.2 Hz and 2.8 Hz, respectively.

On average across the group, the SSD for all test units was ≈ 20% for each of the three different contraction levels/speeds (Suppl. Table 3). The SSD increased for test units recruited near the end of the ascending phase of the contraction (Fig. 10B). There was an effect of recruitment threshold on the SSD values for the 10% [One-way repeated measures ANOVA: $F(6,4) = 28.5$, $p<0.001$], 20% [$F(6,7) = 5.8$, $p < 0.001$] and 30% [$F(6,12) = 7.2$, $p < 0.001$] MVC contraction levels. Post-hoc, SSD values with test units having the lowest recruitment thresholds (0-2% or 2-4% MVC, arrowheads) were significantly smaller than many of the ΔF values having test units with higher recruitment thresholds (marked by stars in Fig. 10B). The highest threshold test units had the largest SSD values whereby 30-40% of their firing occurred when the synaptic input was estimated to be below the recruitment level. These units had the shortest duration of activation during the ascending phase of the contraction (2-3 seconds) and thus, only had to continue to discharge for another 4-6 seconds during the descending phase of the contraction to reach SDD values of ≈ 30%.

< Insert Figure 10 near here >

DISCUSSION

Our results demonstrate that motoneurons recruited over a wide range of force thresholds exhibit evidence of I_P that assist their firing, including producing: a high initial firing rate, accelerated firing shortly after recruitment and self-sustaining firing (ΔF). This extends previous findings of I_P activation in low threshold TA units (D'Amico et al. 2013; Gorassini et al. 2002a; Stephenson and Maluf 2011; Udina et al. 2010) to much higher threshold units. The low and high threshold units, which presumably represent small and large motoneurons respectively, had similar ΔF values even though the I_P in the lower threshold units may be recruited well before firing. This indicates that the portion of the I_P that sustains firing is similar for different sized motoneurons, as was previously demonstrated for rats with both ΔI and ΔF measures (Bennett et al. 2001a; Bennett et al. 2001b; Li et al. 2004). Because the ΔF (or ΔI) estimate of self-sustained firing only estimates the portion of the I_P that is above firing threshold (i.e., tip of the iceberg), the likely subthreshold activation of the I_P in small motoneurons suggests that these neurons may well have larger overall I_P, as detailed further below. Of course, we cannot determine how large the subthreshold I_P is from motor unit firing, but interestingly, a larger I_P in smaller cells is inconsistent with earlier animals studies (Lee and Heckman 1999). However, we now show that motoneuron size (up to the mid-range of sizes, see below) does *not* affect supra-threshold, self-sustained firing in humans, also consistent with previous animals studies (Bennett et al. 2001a; Bennett et al. 2001b; Li et al. 2004).

Motor units decomposed from high-density surface EMG

There are an estimated 445 motor units in the TA muscle (Feinstein et al. 1955) [although potentially less in the older participants (McNeil et al. 2005)], and we were able to decompose 20 of them per participant on average from the HDsEMG using convoluted blind source separation. Because 40%, 55% and 70% of TA motor units are thought to be recruited at 10%, 20% and 30% of MVC

749 respectively (Feiereisen et al. 1997), it is possible that we were able to sample 11%, 8% and 6% of the
750 total population of recruited TA motor units during the 3 contraction levels, respectively. Given that ≈
751 30% of TA muscle fibres are Type II (fast twitch), with pockets located near the surface of the muscle
752 (Henriksson-Larsen et al. 1983; Lexell 1997) where HDsEMG is more likely to decompose larger and
753 superficial units (Farina et al. 2010), it is likely that we decomposed a range of both slow and fast motor
754 units having small and large motoneurons, especially during the 30% MVC contractions where some of
755 the fast superficial motor units may have been activated. However, it is thought that motor units across
756 the TA muscle vary more as a continuum rather than into discrete sub-types. When using HDsEMG to
757 measure conduction velocity across multiple (≈ 40) motor units in the TA muscle, motor units recruited
758 at 30% MVC were in the middle of the full range of conduction velocities and estimated fibre diameters
759 (Del Vecchio et al. 2018). Although we likely sampled motor units in the mid-range of conduction
760 velocities and motoneuron size, we did not recruit the largest and fastest motoneurons which may have
761 different ΔF values to the highest threshold motor units described here (Powers and Heckman 2017).
762 Along with being able to examine multiple motor units, the ability to decompose higher threshold motor
763 units from HDsEMG with high accuracy (≈ 95%) makes this technique advantageous over intramuscular
764 EMG.
765
766 *Comparison of firing properties of motor units from HDsEMG and intramuscular EMG*
767 The firing profiles of the TA motor units decomposed from the HDsEMG exhibited similarities
768 to motor units isolated from intramuscular EMG activated during triangular or trapezoidal dorsiflexions,
769 suggesting that the identification of the decomposed motor units was accurate (Enoka 2019). The fact
770 that the uniquely and blindly identified motor units within the same contraction had firing rate profiles
771 that were temporally modulated together also suggests that the identification of the units was accurate.
772 This also indicated that there was shared synaptic input to all motor units (Farina et al. 2014; Negro et al.

773 2016b) which is important for the ΔF analysis. The start (≈ 8 Hz), maximum (≈ 15 Hz) and end (≈ 6 Hz)
774 firing rates of the decomposed TA motor units were similar to the firing rates of TA motor units
775 identified with intramuscular EMG for similar speeds (1-3% MVC/s) and magnitudes (10-30% MVC) of
776 contraction (D'Amico et al. 2013; Stephenson and Maluf 2011; Udina et al. 2010). Motor units were also
777 detected at recruitment thresholds of < 1% MVC and > 25% MVC for all participants indicating the
778 ability of the HDsEMG to record TA motor units of varying threshold. As discussed further below, the
779 firing rate profiles generated from the decomposed motor units exhibited features such as secondary and
780 tertiary range firing previously described from intracellular motoneuron recordings in response to well
781 controlled, triangular current injection.
782
783 *Secondary range firing*
784 Motor units often display a relatively steep increase in firing rate that lasts for a few seconds
785 after the onset of a contraction (secondary range firing; Fig. 3) (Kiehn and Eken 1997; Udina et al.
786 2010). As shown previously for TA motor units recorded from intramuscular EMG (Erim et al. 1996),
787 we found this prolonged secondary range increased with recruitment order of the motor units, as
788 reflected in the increased slope of the ascending firing rate profile (Fig. 4C). Lower threshold units had a
789 briefer period of secondary range firing compared to the highest threshold units where in the latter, the
790 secondary range sometimes comprised most of the ascending firing rate profile. Secondary range firing
791 is likely due to the acceleration in membrane depolarization produced by the I_P during the onset of firing
792 (Li et al. 2004) as depicted in Figure 1A iv. The briefer secondary range in the lowest threshold units
793 may be due to the I_P being activated well below firing threshold, so by the time the motoneuron begins
794 to fire, the I_P is past its early slow onset and rapidly completing its final activation (in steep range of its
795 I-V relation, Fig. 1B i), giving a rapid boost to firing at recruitment (see details below). In contrast, the
796 I_P activation is likely initiated closer to the firing threshold of the higher threshold units to produce an
797 acceleration in discharge at motor unit recruitment over the first few seconds of firing, as the I_P is slowly

activated over its full range. Typically, the secondary range in these high threshold units lasts for a few seconds which likely reflects the known slow onset of the I_P, which in turn reflects the time it takes for the opening probability of the L-type calcium channels to slowly warmup (via channel dimerization), after which these calcium currents activate much more rapidly (leading to steep region of the I-V relation; Fig. 1B) (Binder et al. 2020).

Tertiary Range Firing

Following the secondary range, increases in the firing rate of a motoneuron in response to a continual increase in synaptic input slows down, leading to a linear low slope (gain) region referred to as the tertiary range (Hultborn et al. 2004; Lee et al. 2003; Li et al. 2004). Tertiary range firing was most prominent in the lowest threshold motor units, partly because they were simply activated for longer, but also because they had a shorter duration of secondary range firing. Although slowed, the firing rate of the motor units continued to increase linearly during increases in effort (synaptic input) in the tertiary range, with peak firing rates occurring near peak torque. Thus, there did not appear to be a large amount of rate saturation or spike accommodation at these speeds (1-3 %MVC/s) and magnitudes (10-30% MVC) of contraction. This is in contrast to firing rate profiles of TA motor units that have much weaker (< 10% MVC) and slower rates of contraction (< 1% MVC/s) (Revill and Fuglevand 2017) or units that are activated for longer periods of time (> 10s) at much higher levels of contraction (> 30% MVC) (Erim et al. 1996). Thus, using contractions with moderately slow speeds (1-3 % MVC/s) and strengths (10-30% MVC) are likely best to keep the firing rate profiles of the motor units linear with respect to their inputs, a requirement for ΔF methods, especially for the lowest threshold units that fire primarily in their tertiary range.

Despite the relatively linear tertiary range firing, the firing rates on the descending phase of the contraction jumped to a lower offset (or sag) but continued with a similar slope as on the ascending phase of the contraction, especially for the low threshold control motor units. This sag is often

observable in the firing frequency profiles of rat motoneurons in response to triangular current injections (Bennett et al. 2001a) or to sinusoidal stretch (Gorassini et al. 1999) and is a convenient marker of when the synaptic input starts to decrease during the descending phase of the contraction, occurring just after peak torque in the human data. The ionic mechanism of the sag is not known but may result from a rate (direction)-dependent effect of the depolarizing drive on spiking (Kuo et al. 2006; Norton et al. 2008), calcium and sodium I_P inactivation (Lee and Heckman 1999; Powers and Heckman 2017) or the buildup of calcium-activated potassium (SK) currents (Li and Bennett 2007). The influence of sag on the ΔF measures are discussed below.

Composite control unit method to estimate self-sustained firing produced by I_P (ΔF)

Because the lowest threshold units had pronounced tertiary range firing that was likely linearly related to the synaptic input profile, we exclusively used them as control units for the ΔF measures. By only using the lowest threshold units as control units, this reduced many underestimation and overestimation errors in the ΔF values as summarized below.

Floor effects (a). The lowest threshold test motor units were recruited when the firing rates of their even lower threshold control unit pair were very low. Thus, there was little room for the control unit in these cases to decrease its rate when the test unit was de-recruited. Using these lowest threshold units only as control and not test units in the composite method helped to reduce the number of very low ΔF values compared to the pairwise method (Fig. 9A).

Non-linear firing of high threshold units (b-d). By only using the lowest threshold motor units as control units also helped to reduce the number of underestimated ΔF values by avoiding the use of higher threshold control units with large secondary range firing which could underestimate synaptic

847 inputs to the test units if they were recruited at the start of the control unit's secondary range. This likely
848 produced many of the low ΔF values for ΔT recruitment times that were < 2 s in the pairwise method.
849 By grouping together the lowest threshold units, the higher threshold test units were typically recruited
850 at a later time when the composite control units were already firing in their linear, tertiary range where
851 synaptic inputs likely were not underestimated.

852 Overestimation of ΔF values could also occur when using higher threshold control units with
853 large accelerations and amplitudes in firing rate at the time of test unit recruitment, indicative of high
854 input-output gain of the motoneuron (Lee and Heckman 1998a; 1999). This was avoided with the
855 composite control method that only employed the firing rate profiles from the lowest threshold (< 3%
856 MVC) motor units as a measure of synaptic input. The ascending slope of the firing rate profiles, which
857 was a good indicator of secondary range firing and high gain, was lower in the composite control profile
858 (< 1 Hz/s) compared to the earliest recruited higher threshold test units (>> 1 Hz/s, Fig. 9B). In addition
859 to the ascending slopes, a high threshold control unit could have a steep decrease in firing rate
860 (descending slope) indicative of secondary range firing during I_P deactivation. If a test unit was de-
861 recruited at this time, it could result in an artificially low estimate of synaptic input which would also
862 produce an overestimated ΔF (Hassan et al. 2019). These overestimations contributed to the continued
863 variability in ΔF values at ΔT recruitment times > 2 s in the pairwise method. In contrast, the shallow,
864 linear ascending and descending slope of the composite control firing profile occurred throughout the
865 majority of the contraction when all of the higher threshold test units were being recruited and de-
866 recruited and thus, avoided the secondary range non-linearity. The firing rate slopes of the composite
867 control units were also similar for the ascending and descending phase of the contraction to ensure that
868 the rate of increase and decrease in depolarizing drive was the same. This is important since the rate of
869 depolarizing drive can affect the activation of the sodium component of the I_P (Kuo et al. 2006).
870

Modulation depth and ΔF

The minimum to maximum excursion in the firing rate of the composite control unit profile (modulation depth or CMod) was larger than the ΔF values measured for the test units, especially for the 20% and 30% MVC contractions where ΔF was typically half of the modulation depth. Thus, there was enough sensitivity in the control unit firing rates to reflect changes in synaptic inputs at these higher levels of contraction. Moreover, unlike the pairwise method [(see also (Hassan et al. 2019; Powers et al. 2008; Stephenson and Maluf 2011)] there was no relationship between ΔF and modulation depth for the composite control unit method, especially for the 20% and 30% MVC contractions. These stronger and faster contractions, unlike the 10% MVC trials, likely produced enough synaptic drive so that the composite control motoneurons had firing rates with linear responses to synaptic inputs in the tertiary range while the test motor units were being recruited and de-recruited. In addition, the higher threshold control units with high modulation depths (CMod) that produced equally large (overestimated) ΔF values in the pairwise method were also removed by the composite control method.

The maximum firing rates reached by some of the composite control units could level off between 20 and 30% MVC due to small amounts of rate saturation. However, the firing rate of the composite control units when the test motor units were recruited were ≈ 2 Hz lower than the maximum firing rates of the composite control units where rate saturation was less likely. Thus, it is recommended that contraction ramps of at least 20-30% MVC over 10 s be used to ensure the modulation depth of the composite control units do not constrain the measurements of ΔF in the test motor units.

Short ascending activation times of test units

Another source of error in estimating the I_P values occurred in test units recruited at the top of the triangular force contractions. These high threshold units were only activated for a couple seconds and likely did not have enough time to fully activated their I_P and stopped firing rapidly on the

descending phase of the contraction with little ΔF (Fig. 8). Animal and human studies have found a similar phenomenon, since the I_P can take seconds to fully activate (Bennett et al. 1998a; Li et al. 2004; Udina et al. 2010), potentially due to warmup related effects (Binder et al. 2020). These same units that exhibited a small ΔF at the top of the contraction ramp exhibited a much larger ΔF when given longer times to fire and activate their I_P in stronger contractions. Thus, it is important to consider the ascending activation time of a test unit when measuring ΔF values in an individual or experimental condition as test units with low ΔF's and short activation times less than 2 s should be considered as a separate population as we did here.

In summary, using a composite control unit profile containing the lowest threshold units with mainly tertiary range firing provided the best representation of synaptic input to the test motor units and thus, a more accurate measure of the self-sustained activation of the motoneuron from the I_P. Although the average ΔF did not change when using only the lowest threshold units in the composite control profile, compared to using all possible motor units as controls in the pairwise method, the variability of ΔF values was decreased by half, which is important when comparing self-sustained firing across groups or in response to an intervention that might have a small effect size. In this study, we purposefully kept all unit pairs with short ΔT recruitment times and close ΔF and CMod values in both methods to illustrate how the composite method naturally eliminates these problematic pairings. Even so, the pairwise ΔF remained more variable compared to the composite ΔF for unit pairs with ΔT recruitment times > 2s because of the overestimation of ΔF from the high threshold control motor units, which also contributed to the ΔF-CMod correlations. Lastly, the control motor units had very similar firing rate profiles so that only one of these control units would likely produce similar ΔF values as the entire composite profile. This needs to be studied in the future and will be important to investigate when fewer numbers of very low threshold motor units can be decomposed from HDsEMG, as may occur in other muscles (Del Vecchio A 2020) and in children (personal observation).

Small motoneurons may have a larger subthreshold I_P than large motoneurons

While the ΔF estimate alone only provides us with information about the contribution of I_P to cell firing, we next consider how changes in the secondary range might help us assess the subthreshold activation of the I_P in different sized motor units (motoneurons). Considering our central finding that the portion of the I_P that sustains firing (ΔF) is invariant with motoneuron size, it is odd that the larger higher threshold motoneurons seem to have a more prolonged activation of the I_P after firing onset, as reflected by their prolonged secondary range. We suggest that this is because these large motoneurons have a smaller overall I_P compared to low threshold motoneurons, but most of it is activated above the firing threshold, including the early portion of the I_P onset that only slowly turns on due to warmup as we detail below (Bennett et al. 1998a; Binder et al. 2020; Svirskis and Hounsgaard 1997). Specifically, during ramp contractions the higher threshold, larger motoneurons start firing at a low frequency relative to where tertiary range firing starts (at blue dot in Fig. 11B, middle trace) and then firing increases relatively steeply but relatively slowly over 2-3 seconds, presumably as the I_P activates slowly over this time (green trace). This relatively slow I_P activation gives rise to a prolonged secondary range (pink shaded area), prior to tertiary range firing when the I_P is fully activated. Importantly, the calcium portion of the I_P takes seconds to active when it starts from its resting state, due to the slow activation of I_P warmup (Bennett et al. 1998a; Svirskis and Hounsgaard 1997), likely via channel dimerization (Binder et al. 2020). Thus, the slow activation of the I_P in high threshold human motoneurons (and prolonged secondary range) suggests that these motoneurons are recruited mainly with their I_P starting in the resting state, and then the I_P warms up slowly over the next few seconds during firing, leading to the prolonged secondary range firing (depicted schematically by shaded pink box over I_P activation period in Fig. 11B). This also suggests that there is not an appreciable amount of I_P activation prior to recruitment (no downward deflection of I_P before firing) and thus, the full I_P contributes to the self-sustained firing, making ΔF faithfully reflect the I_P (marked by ΔI, length of green arrow, Fig. 11B).

943 *< Insert Figure 11 near here >*

944 In contrast lower threshold, smaller human motoneurons start firing with a relatively higher
945 initial rate, just prior to or directly in their tertiary range, where the I_P is nearly fully activated and with
946 much briefer secondary range firing (depicted schematically by purple shading in Fig. 11A, middle
947 trace). The I_P activation during initial firing thus appears to occur more rapidly (during steep I_P slope in
948 Fig. 11A), within the first interspike interval or so (within < 1s), leading to the high initial firing rates. In
949 cat motoneurons warmup of the I_P by a prior activation (within 6 s) leads to a very similar firing pattern,
950 with I_P activation occurring more rapidly (fully activated near recruitment), with tertiary range firing
951 starting at or soon after recruitment, and self-sustained firing still continuing well after the recruitment
952 current [(ΔI; see Fig. 3 in (Bennett et al. 1998a)]. Thus, low threshold human motoneurons behave as
953 though they are warmed up at recruitment. This is most likely due to a substantial subthreshold I_P
954 activation (note downward deflection of I_P before firing, Fig. 11A) that gives enough time prior to
955 recruitment for the I_P to warmup, potentially via calcium channel dimerization (Binder et al. 2020).
956 When calcium channels are warmed up they activate faster, and this leads to a steeper activation of the
957 I_P (at left blue dot in Fig. 11A; steeper I-V relation) so that if a motoneuron is recruited during this steep
958 region, it exhibits much briefer secondary range firing (purple shading, Fig. 11A). The briefer secondary
959 range firing does not necessarily mean there is less I_P activated during firing; instead the I_P is just
960 activated faster and cell firing is initiated closer to the end of the I_P accelerated onset. Presumably, if
961 warmup is indeed important for shaping I_P activation and self-sustained firing in low threshold
962 motoneurons, then varying the contraction speed and intervals between contractions, using previous
963 methods (Gorassini et al. 2002b; Hornby et al. 2003), should change the degree of secondary range and
964 self-sustained firing, a topic we are investigating in future studies.

965 While we found that the ΔF is similar in small and large human motoneurons, as was found for
966 both ΔF and ΔI values in rats (Bennett et al. 2001a; Bennett et al. 2001b; Li et al. 2004), a greater

967 subthreshold I_P activation in small motoneurons suggests that overall these motoneurons have a larger I_P
968 since only the portion of the I_P activated during firing contributes to the ΔF (see schematic in Fig 11).
969 This allows the small portion of the I_P that is activated rapidly at and just after recruitment in small
970 motoneurons (Fig. 11A) to be the same size as the entire I_P that is activated slowly during firing in larger
971 motoneurons (Fig 11B), yielding similar self-sustained firing (ΔF) in small and large motoneurons,
972 though more prolonged secondary range firing in the latter. This highlights a limitation of the ΔF
973 technique in that it can only measure the contribution of the I_P to self-sustained firing during cell firing
974 and any sub-threshold activation of the I_P remains hidden to this measurement. Interestingly, our
975 conclusion that small motoneurons in the human may have larger I_P is opposite to the slightly larger
976 initial I_P peak observed in larger motoneurons of cats (Lee and Heckman 1999) and requires further
977 study.
978
979 *Self-sustained firing duration (SSD)*
980 The SSD provides a functional measure of how much longer I_P keep the motoneuron firing after
981 the synaptic input that initiated the firing is removed. It is not a direct measure of the amplitude of the I_P
982 or the ΔF but only an indication of the proportion of firing that occurs during the self-sustained firing
983 period (the latter defined as firing occurring at levels of synaptic input below that initially needed for
984 recruitment). The amount of self-sustained firing was greater in the higher threshold units that were
985 recruited towards the end of the ascending phase of the contraction (Fig. 10B). These high threshold
986 units fired briefly (2-3 seconds) on the ascending phase of the contraction and only had to fire for
987 another 4-6 seconds on the descending phase of the contraction to produce the comparatively larger SSD
988 values of ≈ 30% (here, the duration of self-sustained firing is 2-3 seconds). This is in comparison to the
989 lower threshold units with longer ascending activation times and thus, a reduced room to fire for very
990 much longer beyond the synaptic recruitment level before the end of the contraction. Thus, the SSD is

991 influenced by the constraints of the triangular contraction profile (and thus not a robust indicator of I_P
992 amplitude) but may still be a useful indication of I_P activation when only examining the firing rate
993 profile of a single motor unit.
994
995 *Limitations and Future Directions*
996 While we conclude that the portion of the I_P that sustains firing is invariant across different sized
997 motor units up to mid-range, this opens up the question of how this occurs as presumably calcium and
998 sodium channel properties have to scale with motoneuron size to achieve this remarkable invariance.
999 Alternatively, the ΔF method may be in some way flawed, and the onus is on future animal and
1000 computer modelling studies to sort this issue out.
1001 Although the composite control method is an improvement over the pairwise method, some
1002 limitations remain. As mentioned in the Methods, the 5^{th} order polynomial line smoothed the firing rate
1003 profile so that the peak of the fit line was shifted to the left of the actual peak of the firing rate. However,
1004 this did not appreciably affect the estimated control unit frequency at recruitment and de-recruitment of
1005 the test unit. In the future, we will determine a more accurate fitting method to represent the peak firing
1006 rate of the units. In addition, instead of using a best straight line fit to measure the entire ascending and
1007 descending slope of the firing rate profile, we will separately identify and calculate the slopes of the
1008 secondary and tertiary ranges, using a bilinear regression fit, to more accurately measure their
1009 amplitudes and durations. The area beneath the secondary range may provide an estimate of the
1010 amplitude of the I_P during its supra-threshold activation time. Lastly, we will examine more closely the
1011 frequency drop (sag) during the descending phase of the contraction. The sag in the composite control
1012 unit profile may affect the ΔF but this effect may be small given that the test units also have a similar
1013 amount of sag.
1014

General summary:

The multiple motor units decomposed from HDsEMG displayed different firing behaviours whereby the lowest threshold units fired primarily in the tertiary range indicative of appreciable I_P recruitment subthreshold to firing, whereas higher threshold units had more prolonged secondary range firing indicative of continued I_P activation after recruitment. By using only the lowest threshold units in the composite control unit method, the firing rate profiles provided a more accurate representation of synaptic inputs to the TA motoneuron pool given the more linear and proportional relationship of firing rate to synaptic input in the tertiary range. Thus, the composite control unit method avoids under and overestimating ΔF values that occur when using higher threshold control unit firing profiles with substantial secondary range firing during both recruitment and de-recruitment. The composite control profiles had a large enough firing rate modulation to not constrain the ΔF values but only when the synaptic drive was large enough in the 20% and 30% MVC trials. Contraction rates of 2 and 3% MVC/s over 10 seconds to these force levels did not produce appreciable firing rate accommodation or saturation. Interestingly, ΔF values were similar across test units of different recruitment thresholds that were activated by small and large motoneurons, respectively, indicating that the portion of the I_P that sustains firing is similar for all motoneurons. These conclusions could not have been reached with the large variability in the conventional pairwise unit analysis, and required our new composite control method and elimination of ΔF estimation errors we have detailed. Overall, we recommend that using contraction strengths of 20 to 30% MVC and firing rates of the lowest threshold units likely provide the best representation of synaptic drive to test motor units for the accurate measurement of ΔF and self-sustained firing mediated by the I_P.

FIGURE LEGENDS

Figure 1. Synaptic and intracellular I_P activation and self-sustained firing. A) Synaptic activation of cat soleus motoneuron by sinusoidal muscle stretch. **i-iii)** Firing response of the motoneuron to muscle stretch (synaptic input) when spiking was slightly impeded (- 1 nA, i), not altered (0 nA, ii) or aided (+1 nA, iii) with steady somatic current injection that does not much alter the distal dendritic I_P, as detailed and modified from (Bennett et al. 1998b). Self-sustained firing (pink shading) increased as more of the I_P was activated above the firing threshold (iii). **iv)** Membrane potential response to stretch during hyperpolarization to estimate the synaptic input (grey trace) and membrane potential at rest to estimate the contribution of the I_P (green), which here is a plateau potential because spikes are blocked with QX314 (different cell from i-iii, smoothed). **v)** Membrane potential response to stretch during hyperpolarization to estimate the synaptic input in the same cell as i - iii (black trace), and with trace from iv overlaid (grey). **vi)** Firing response of motoneuron where I_P is activated before recruitment due to prior activation (warmup). **vii)** Firing response of tonically firing motoneuron with tonic I_P activation. Firing response is proportional to synaptic stretch input profile (grey trace). Dashed vertical line in iv-vi marks the end of synaptic stretch input. **B) i)** Top trace: membrane potential of low threshold motoneuron during spiking in response to triangular injected current (black trace). I_P activation is marked by small acceleration in potential just before onset of firing. Bottom trace: firing duration marked by purple box where firing starts at higher current and stops at lower current (blue circles, the difference is ΔI). Firing starts after majority of I_P (green trace with depolarizing inward current depicted in downward direction) is activated, producing a small ΔI (length of black arrow). **ii-iii)** Likely firing responses of two other hypothetical motoneurons (same as in i) but with more of the I_P activated during firing (spike threshold lower relative to I_P onset) to produce a larger ΔI. **iv)** Voltage clamp command (black trace) and resulting I_P without (green) and with (grey) sag in I_P, estimated for motoneuron in part i; Figure modified from (Li et al. 2004). Dashed line indicates turn around point of current and start of

I_P sag. **v)** Firing-current response to triangular current injection displaying primary (black), secondary (pink, during I_P activation) and tertiary (green, after I_P activation) firing ranges. Figure modified from (Li et al. 2004).

Figure 2. Parameters measured from the motor unit firing rate profile.

A) Top trace: torque profile for a 20% MVC contraction showing recruitment threshold of the motor unit. **Second trace:** corrected firing rate profile (blue dots) of decomposed motor unit (see below for details). Straight line fit to the secondary (pink) and tertiary (green) firing range. Time of peak firing rate is marked by vertical dashed line and denotes start of lower offset (sag) in firing rate during the descending phase of the contraction. **Third trace:** Uncorrected firing rate profile. The 5^{th} order polynomial line fit to the firing rate profile is marked with a green line where the coefficient of determination (R^2) of the fit was measured. The straight line fit to the data points on the entire ascending and descending portion of the polynomial line is marked with a dashed pink line from which the ascending and descendng slope values were measured, respectively. Black downward arrows mark the start and end firing rates measured from the polynomial line. Modulation depth (MoD) is the maximum rate - the minimum rate measured from the polynomial line. **Bottom trace:** The train of pulse amplitudes (blue lines) from the decomposition algorithm (marking firing times of the decomposed motor unit) with an accuracy (silouette) value of 0.94. Red circles mark pulses selected by the blind source algorithm and black circles mark pulses that were not selected, producing abnormally low firing rate values marked by small black arrows in the firing rate profile of the third trace. The dashed blue arrows point to the re-estimated pulses (dotted red circles) following recomputation of the pulse train to include the missed pulses. The resulting corrected firing rate profile after the recalculation/re-estimation is plotted in the second trace. Data from participant 4M. **B-D)** Average number of motor units decomposed from HDsEMG per contraction **(B)**, accuracy (sillouette) values **(C)** and coefficient of

1085 determination (R^2) of the polynomial line fit to frequency profile **(D).** Average of the mean values from
1086 each of the 7 participants at the 10%, 20% and 30% MVC trials. Individual data presented in
1087 Supplemental Table 1. Error whiskers +1 standard deviation (SD).
1088
1089 **Figure 3. Firing profiles of multiple motor units and ΔF calculation. A)** Firing rate profiles of 19
1090 decomposed motor units during a 22% MVC contraction (participant 1F) in ascending order of
1091 recruitment threshold over 2 columns (same torque trace over each column). Dashed vertical line marks
1092 peak discharge rates at turnaround of torque. Pink and green lines mark secondary and tertiary range
1093 firing in Units 1 and 10, respectively. Lower green line marks sag during descending phase. Short
1094 horizontal coloured lines mark 0 Hz baseline for each rate profile. **B. Left:** Overlay of polynomial lines
1095 from the 19 motor units in A (participant 1F) using the same colour coding. **Right:** Similar polynomial
1096 lines from participant 5M during a 30% MVC contraction. **C) Left:** Paired unit analysis for Units 1
1097 (control) and Unit 2 (test) from A with ΔF of 1.1 Hz. **Right:** Unit 1 (control) vs Unit 9 (test) producing
1098 ΔF of 3.7 Hz. Dashed vertical lines mark recruitment and de-recruitment of test units. **D)** Same as in C
1099 but for test Unit 17 paired with control Unit 13 **(left)** and control Unit 6 **(right)** producing ΔF of -0.3 Hz
1100 and 5.3 Hz, respectively. **E)** ΔF values for each test unit in A using same rainbow colour code, plotted
1101 against recruitment threshold. Number of control units paired with each test unit increases with
1102 recruitment order to produce progressively larger number of ΔF values. Test units in C and D (U2, U9
1103 and U17) are marked in plot.
1104
1105 **Figure 4. Ascending and Descending Rate Slopes, Start, End and Maximum Rates. A)** Group average
1106 across all 7 participants for ascending **(i)** and descending **(ii)** slope of polynomial line fit through the
1107 firing rate profile at all contraction strengths (* p all < 0.05 when comparing ascending and descending
1108 slope at each contraction level). **B)** Group average of start, end and maximum rates for each contraction

level taken from the fit polynomial line. * $p < 0.01$ between start and end rates. **C) Left graphs:** Slope of the ascending firing rate of a motor unit plotted against its recruitment threshold from all test units for the 6 contractions at the 10%, 20% and 30% MVC contraction strenghts. Data from participant 7F. Red line is the straight line fit to the data. **Right graph:** Group average of slope of straight line fit through the ascending slope vs recruitment threshold data. **D)** Same as in C but for data during the descending phase of the contraction. Average slope values in C and D (right graphs) all greater than 0 (p all < 0.001) but not different from each other ($p > 0.05$). Data in C and D (left graphs) taken from participant 7F who on some trials overshot the 20% MVC target by 5%. Individual participant data in Supplemental Table 1. Error whiskers +1 SD.

Figure 5. ΔF from Pairwise and Composite Control Methods. A) ΔF values obtained from the pairwise method plotted against ΔT recruitment times for 10, 20 and 30% MVC trials from participant 1F. Red line indicates best fit from exponential rise to maximum. Number of ΔF values indicated in lower right of each graph. **B)** Same as in A but for ΔF values measured from composite control method. Best fit straight line in red. **C)** ΔF values for pairwise (Pair) and composite control (Comp) method for 10, 20 and 30% MVC trials in A and B respectively. Mean represented by the red line which covers the black median line, the 25th and 75th percentiles by the box bounds, and the 95th and 5th percentiles by the whiskers. Open circles represent outliers. **D)** Comparison of mean ΔF values across the 7 participants for the pairwise (black bars) and composite control (red bars) method and composite control without ΔF values from test units having short ascending activation (SA) times (see Fig. 8 for details on SA units). **E)** Coefficient of variation (CoV) for the different mean ΔF values as in D. * $p < 0.005$. Individual participant data in Supplemental Table 2. Error whiskers +1 SD.

Figure 6. Composite Control Motor Unit Profile. A) Overlay of firing frequency profiles of Unit 1 (pink circles), Unit 2 (blue-green circles) and Unit 3 (light blue circles) from Figure 3A. Slope of secondary and tertiary range firing is marked by pink and green lines, respectively. **B)** Same plot as in A but with the frequency points in the secondary range removed. A new 5^{th} order polynomial line was fit to the edited profile (red line). Removing the frequency points in the secondary range made the slope of the ascending frequency profile (0.74) similar to the slope of the descending frequency profile (-0.72). The slope values were measured from a straight line fit to the polynomial line. **C and D)** Paired unit analysis using test units U17 and U4 from Figure 3 paired against the composite control unit profile (Comp). **E-H)** Mean ratio of the ascending and descending firing rate slope for the composite control profiles **(E)**, mean R^2 value of the control rate-test rate plots **(F)**, mean number of motor units in the composite control unit profile **(G),** and mean number of unit pairs in the ΔF analysis **(H):** average of mean values from each of the 7 participants for the 10, 20 and 30% MVC trials. In F and H, data displayed for the pairwise (black bars), composite control (red) and composite control without SA test units (green). Individual participant data in Supplementary Tables 2 and 3. Error whiskers +1 SD.

Figure 7. ΔF and Control Unit Modulation for Pairwise and Composite Control Unit Methods. Ai) ΔF values of all 6 contractions plotted against control unit modulation (CMod) for the pairwise ΔF method in participant 5M at the 10, 20 and 30% MVC trials. Black line marks the line of unity where ΔF = Cmod values. Pearson's product correlation coefficient (r) and the significance of the correlation are indicated in top left of each graph for the ΔF and CMod relationship. Red line denotes straight line fit to the data. **ii)** Same as in Ai but for ΔF measured with the composite control unit method. **B)** Maximum firing rate of the composite control unit profile ($CMax_{comp}$) measured from the polynomial line at the 10, 20 and 30% MVC trials for participant 5M. Median and mean represented by black and red line, the 25th and 75th percentiles by the box bounds, and the 95th and 5th percentiles by the whiskers. **C)** Same

as in B but for the firing rate of the composite control motor unit when the test motor unit was recruited ($C_{comp}RT$). **D)** Group data for the Composite Control Unit Method: composite control unit modulation depth (CMod, black bars), ΔF values (red bars), maximum rate of the composite control unit profile (CMax, dark green bars) and composite control unit rate when the test unit was recruited (C_RT, light green bars) averaged across the 7 participants for the 10, 20 and 30% MVC trials. **E)** Average slope of the straight line fit to the ΔF vs Cmod data (red lines in A) for the pairwise (black bars) and composite control unit (red bars) method across the 7 participants. * indicates difference from a slope of 0, $p < 0.025$. Individual participant data for D and E in Supplemental Table 2. Error whiskers +1 SD.

Figure 8. Test units with short ascending activation (SA) times. Ai) Test unit (dark grey circles) paired with composite control motor unit profile (multi-colour circles) in participant 6M for a 30% MVC contraction. The test unit was recruited at 13% MVC (torque top trace) and discharged for 3.6 s during the ascending phase of the firing rate profile. The ΔF value from this test unit (5.7 Hz) is plotted in B as one of the dark grey circles because it was activated for > 2 seconds on the ascending phase of the contraction. **Aii and iii)** Same as in Ai but for two test units (red circles) that were recruited > 20% MVC and with durations of firing during the ascending frequency profile that were < 2s, i.e., having short ascending activation (SA) times. The ΔF values for these 2 test units are plotted with red circles in B. **B)** All ΔF and recruitment threshold values from the 6 contractions at 30% MVC in participant 6M. **C-D)** ΔF values from this same participant plotted against recruitment torque at the 20% MVC **(C)** and 10% MVC **(D)** trials. ΔF values marked with red circles have test units with SA times and ΔF < -1 SD. ΔF measures with test units having SA times removed from the average are shown in Figures 5 and 6.

Figure 9. ΔF and test motor unit recruitment threshold. A) Binned average of ΔF values across the 7 participants plotted against recruitment threshold of the test unit for the 10%, 20% and 30% MVC data.

Bin widths are 2% MVC wide. Green circles mark ΔF values from composite control unit method and black circles mark ΔF values from pairwise method. * indicate ΔF values that are different from the ΔF value at the 0-2% MVC bin (arrowhead) for the pairwise data (no bins were different in the composite control data). Missing ΔF value for test units having recruitment thresholds between 28-30% MVC in the composite 30% MVC data due to a small number of values for this bin. Test units with SA times were removed from dataset. **B)** Binned average for the slope of the ascending firing rate profile of the test motor units. Same format as in A. Grey bars represent the equivalent of every 2 seconds in time for the 10 s ascending contraction in each of the different contraction strengths. Error whiskers ± 1 SD.

Figure 10. Self-sustained firing duration (SSD). A) Examples of test - composite control unit pairs from participant 3M during a 30% MVC trial. **i)** Test unit with large self-sustained firing duration (SSD) index and **ii)** test unit with small SSD. Vertical gray lines mark the time that the estimated synaptic input reached level that recruited test unit during the ascending (a) and descending (a^1) phase of contraction. The duration of a = time of test unit recruitment to time of peak synaptic input (torque), the latter marked by the dashed vertical line. The duration of a^1 is estimated by the duration of a. Solid black vertical line marks time of de-recruitment of test unit. Distance between right grey vertical line and solid black line indicates duration of self-sustained firing of unit, i.e., duration of time unit fires below synaptic input initially needed to recruit unit (see calculation in text). ΔF values calculated as in Figure 3. **B)** SSD of test units averaged for the 7 participants plotted against recruitment threshold at each contraction intensity (10, 20 and 30% MVC). Bin width 2% MVC. Missing values in 20% and 30% MVC data due to small number of samples for the lowest and highest threshold units (many of the lowest threshold units were used as control units and some high threshold SA units were removed). *'s indicate SSD values that are different from the SSD value at the 0-2% MVC bin or 2-4% MVC bin

(arrowhead). Grey bars represent the equivalent of every 2 seconds in time for the 10 s ascending contraction for the different contraction strengths. Error whiskers ± 1 SD.

Figure 11. I_P activation and ΔI in low and high threshold motoneurons. A) Top trace: membrane potential of hypothetical low threshold (small) motoneuron during spiking in response to triangular injected current, but used to schematically represent firing in our voluntary ramp contractions. **Middle traces:** schematic representation of the synaptic input (downward depolarizing current) and I_P current (green trace) activated during the contraction. Firing duration marked by purple box where firing starts at higher current and stops at lower current (blue circles, the difference is ΔI). A large portion of I_P is activated prior to cell firing, giving time for the I_P to be warmed up, so the current changes steeply at the onset of firing leading to only a brief secondary range (light purple rectangle). Only the portion of the I_P activated after firing contributes to the ΔI (length of green arrow). Data adapted from (Li et al. 2007) to schematically demonstrate the contribution of the I_P to the ΔF and ΔI. **B) Top trace:** membrane potential of hypothetical high threshold (large) motoneuron during spiking in response to triangular injected current, as in A; adapted from (Li et al. 2007). **Middle trace:** firing duration marked by red box where firing starts at higher current and stops at lower current (blue circles, the difference is ΔI). I_P (green trace) is at rest prior to cell firing and this non-warmed up I_P has a slow onset, leading to a prolonged secondary range after onset of firing. The entire I_P contributes to the ΔI (length of green arrow). Overall I_P in high threshold motoneuron is smaller than in low threshold motoneuron but the amount of the I_P contributing to ΔI (and ΔF) is the same.

SUPPLEMENTAL MATERIAL

Supplemental Tables are located in the Figshare data repository:

https://doi.org/10.6084/m9.figshare.12067344.

GRANTS

This work was supported by a National Institute of Neurological Disorders and Stroke Grant R01 NS-104436 to K.A.Q., a National Science and Engineering Grant 05205 to M.A.G. and post-doctoral fellowships to B.A. from the Women and Children's Health Research Institute and the Neuroscience and Mental Health Institute at the University of Alberta.

DISCLOSURES

No conflicts of interest, financial or otherwise, are declared by the authors.

ACKNOWLEDGEMENTS

We thank Tia Bennett for editing the manuscript.

AUTHOR CONTRIBUTIONS

B.A., K.A.Q. and **M.A.G.** conceived and designed research; **B.A., J.D., K.F.** and **M.A.G.** performed experiments; **B.A., N.M., J.D.** and **M.A.G.** analyzed data; **C.T. and F.N.** advised on decomposition analysis; **B.A., D.J. B.** and **M.A.G.** interpreted results of experiments; **B.A., D.J.B. and M.A.G.** prepared figures; **B.A., D.J.B., F.N.** and **M.A.G.** drafted manuscript; **B.A., K.F., D.J.B.** and **M.A.G.** edited and revised manuscript; **B.A., N.M., K.F., C.T., F.N., K.A.Q., D.J.B.** and **M.A.G.** approved final version of manuscript.

REFERENCES

Bennett DJ, Hultborn H, Fedirchuk B, and Gorassini M. Short-term plasticity in hindlimb motoneurons of decerebrate cats. *J Neurophysiol* 80: 2038-2045, 1998a.

Bennett DJ, Hultborn H, Fedirchuk B, and Gorassini M. Synaptic activation of plateaus in hindlimb motoneurons of decerebrate cats. *J Neurophysiol* 80: 2023-2037, 1998b.

Bennett DJ, Li Y, Harvey PJ, and Gorassini M. Evidence for plateau potentials in tail motoneurons of awake chronic spinal rats with spasticity. *J Neurophysiol* 86: 1972-1982, 2001a.

Bennett DJ, Li Y, and Siu M. Plateau potentials in sacrocaudal motoneurons of chronic spinal rats, recorded in vitro. *J Neurophysiol* 86: 1955-1971, 2001b.

Binder MD, Powers RK, and Heckman CJ. Nonlinear Input-Output Functions of Motoneurons. *Physiology (Bethesda)* 35: 31-39, 2020.

Boccia G, Martinez-Valdes E, Negro F, Rainoldi A, and Falla D. Motor unit discharge rate and the estimated synaptic input to the vasti muscles is higher in open compared with closed kinetic chain exercise. *J Appl Physiol (1985)* 127: 950-958, 2019.

Carlin KP, Jones KE, Jiang Z, Jordan LM, and Brownstone RM. Dendritic L-type calcium currents in mouse spinal motoneurons: implications for bistability. *Eur J Neurosci* 12: 1635-1646, 2000.

D'Amico JM, Murray KC, Li Y, Chan KM, Finlay MG, Bennett DJ, and Gorassini MA. Constitutively active 5-HT2/alpha1 receptors facilitate muscle spasms after human spinal cord injury. *J Neurophysiol* 109: 1473-1484, 2013.

Del Vecchio A HA, Falla D, Felici F, Enoka RM, and Farina D. Tutorial: Analysis of motor unit discharge characteristics from high-density surface EMG signals. *Journal of Electromyography and Kinesilogy* https://doi.org/10.1016/j.jelekin.2020.102426: 2020.

Del Vecchio A, Negro F, Felici F, and Farina D. Distribution of muscle fibre conduction velocity for representative samples of motor units in the full recruitment range of the tibialis anterior muscle. *Acta Physiol (Oxf)* 222: 2018.

Desmedt JE, and Godaux E. Ballistic contractions in man: characteristic recruitment pattern of single motor units of the tibialis anterior muscle. *J Physiol* 264: 673-693, 1977.

Elbasiouny SM, Bennett DJ, and Mushahwar VK. Simulation of Ca2+ persistent inward currents in spinal motoneurones: mode of activation and integration of synaptic inputs. *J Physiol* 570: 355-374, 2006.

Enoka RM. Physiological validation of the decomposition of surface EMG signals. *J Electromyogr Kinesiol* 46: 70-83, 2019.

Erim Z, De Luca CJ, Mineo K, and Aoki T. Rank-ordered regulation of motor units. *Muscle Nerve* 19: 563-573, 1996.

Farina D, Holobar A, Merletti R, and Enoka RM. Decoding the neural drive to muscles from the surface electromyogram. *Clin Neurophysiol* 121: 1616-1623, 2010.

Farina D, Negro F, and Dideriksen JL. The effective neural drive to muscles is the common synaptic input to motor neurons. *J Physiol* 592: 3427-3441, 2014.

Feiereisen P, Duchateau J, and Hainaut K. Motor unit recruitment order during voluntary and electrically induced contractions in the tibialis anterior. *Exp Brain Res* 114: 117-123, 1997.

Feinstein B, Lindegard B, Nyman E, and Wohlfart G. Morphologic studies of motor units in normal human muscles. *Acta Anat (Basel)* 23: 127-142, 1955.

Freund HJ. Motor unit and muscle activity in voluntary motor control. *Physiol Rev* 63: 387-436, 1983.

Fuglevand AJ, Lester RA, and Johns RK. Distinguishing intrinsic from extrinsic factors underlying firing rate saturation in human motor units. *J Neurophysiol* 113: 1310-1322, 2015.

Gorassini M, Bennett DJ, Kiehn O, Eken T, and Hultborn H. Activation patterns of hindlimb motor units in the awake rat and their relation to motoneuron intrinsic properties. *J Neurophysiol* 82: 709-717, 1999.

Gorassini M, Yang JF, Siu M, and Bennett DJ. Intrinsic activation of human motoneurons: possible contribution to motor unit excitation. *J Neurophysiol* 87: 1850-1858, 2002a.
Gorassini M, Yang JF, Siu M, and Bennett DJ. Intrinsic activation of human motoneurons: reduction of motor unit recruitment thresholds by repeated contractions. *J Neurophysiol* 87: 1859-1866, 2002b.
Gorassini MA, Bennett DJ, and Yang JF. Self-sustained firing of human motor units. *Neurosci Lett* 247: 13-16, 1998.
Hassan AS, Thompson CK, Negro F, Cummings MQ, Powers RK, Heckman CJ, Dewald J, and McPherson LM. Impact of parameter selection on estimates of motoneuron excitability using paired motor unit analysis. *J Neural Eng* 2019.
Heckman CJ, Johnson M, Mottram C, and Schuster J. Persistent inward currents in spinal motoneurons and their influence on human motoneuron firing patterns. *Neuroscientist* 14: 264-275, 2008.
Heckmann CJ, Gorassini MA, and Bennett DJ. Persistent inward currents in motoneuron dendrites: implications for motor output. *Muscle Nerve* 31: 135-156, 2005.
Henriksson-Larsen KB, Lexell J, and Sjostrom M. Distribution of different fibre types in human skeletal muscles. I. Method for the preparation and analysis of cross-sections of whole tibialis anterior. *Histochem J* 15: 167-178, 1983.
Hermens HJ, Freriks B, Disselhorst-Klug C, and Rau G. Development of recommendations for SEMG sensors and sensor placement procedures. *J Electromyogr Kinesiol* 10: 361-374, 2000.
Holobar A, and Farina D. Blind source identification from the multichannel surface electromyogram. *Physiol Meas* 35: R143-165, 2014.
Holobar A, Minetto MA, and Farina D. Accurate identification of motor unit discharge patterns from high-density surface EMG and validation with a novel signal-based performance metric. *J Neural Eng* 11: 016008, 2014.
Hornby TG, Rymer WZ, Benz EN, and Schmit BD. Windup of flexion reflexes in chronic human spinal cord injury: a marker for neuronal plateau potentials? *J Neurophysiol* 89: 416-426, 2003.
Hounsgaard J, Hultborn H, Jespersen B, and Kiehn O. Bistability of alpha-motoneurones in the decerebrate cat and in the acute spinal cat after intravenous 5-hydroxytryptophan. *J Physiol* 405: 345-367, 1988.
Hultborn H, Brownstone RB, Toth TI, and Gossard JP. Key mechanisms for setting the input-output gain across the motoneuron pool. *Prog Brain Res* 143: 77-95, 2004.
Johnson MD, Thompson CK, Tysseling VM, Powers RK, and Heckman CJ. The potential for understanding the synaptic organization of human motor commands via the firing patterns of motoneurons. *J Neurophysiol* 118: 520-531, 2017.
Kiehn O, and Eken T. Prolonged firing in motor units: evidence of plateau potentials in human motoneurons? *J Neurophysiol* 78: 3061-3068, 1997.
Kuo JJ, Lee RH, Zhang L, and Heckman CJ. Essential role of the persistent sodium current in spike initiation during slowly rising inputs in mouse spinal neurones. *J Physiol* 574: 819-834, 2006.
Lee RH, and Heckman CJ. Adjustable amplification of synaptic input in the dendrites of spinal motoneurons in vivo. *J Neurosci* 20: 6734-6740, 2000.
Lee RH, and Heckman CJ. Bistability in spinal motoneurons in vivo: systematic variations in persistent inward currents. *J Neurophysiol* 80: 583-593, 1998a.
Lee RH, and Heckman CJ. Bistability in spinal motoneurons in vivo: systematic variations in rhythmic firing patterns. *J Neurophysiol* 80: 572-582, 1998b.
Lee RH, and Heckman CJ. Enhancement of bistability in spinal motoneurons in vivo by the noradrenergic alpha1 agonist methoxamine. *J Neurophysiol* 81: 2164-2174, 1999.
Lee RH, Kuo JJ, Jiang MC, and Heckman CJ. Influence of active dendritic currents on input-output processing in spinal motoneurons in vivo. *J Neurophysiol* 89: 27-39, 2003.

Lexell J. Muscle capillarization: morphological and morphometrical analyses of biopsy samples. *Muscle Nerve Suppl* 5: S110-112, 1997.
Li X, and Bennett DJ. Apamin-sensitive calcium-activated potassium currents (SK) are activated by persistent calcium currents in rat motoneurons. *J Neurophysiol* 97: 3314-3330, 2007.
Li X, Murray K, Harvey PJ, Ballou EW, and Bennett DJ. Serotonin facilitates a persistent calcium current in motoneurons of rats with and without chronic spinal cord injury. *J Neurophysiol* 97: 1236-1246, 2007.
Li Y, Gorassini MA, and Bennett DJ. Role of persistent sodium and calcium currents in motoneuron firing and spasticity in chronic spinal rats. *J Neurophysiol* 91: 767-783, 2004.
Martinez-Valdes E, Laine CM, Falla D, Mayer F, and Farina D. High-density surface electromyography provides reliable estimates of motor unit behavior. *Clin Neurophysiol* 127: 2534-2541, 2016.
Martinez-Valdes E, Negro F, Farina D, and Falla D. Divergent response of low- versus high-threshold motor units to experimental muscle pain. *J Physiol In press,* 2020.
Martinez-Valdes E, Negro F, Laine CM, Falla D, Mayer F, and Farina D. Tracking motor units longitudinally across experimental sessions with high-density surface electromyography. *J Physiol* 595: 1479-1496, 2017.
McNeil CJ, Doherty TJ, Stashuk DW, and Rice CL. Motor unit number estimates in the tibialis anterior muscle of young, old, and very old men. *Muscle Nerve* 31: 461-467, 2005.
Merletti R, Farina, D. editor. *Chapter 3. Detection and Conditioning of Surface EMG Signals. Surface Electromyograph: Physiology, Engineering, and Applications.* Piscataway,NJ: John Wiley & Sons, Inc., 2016, p. 54-90.
Negro F, Muceli S, Castronovo AM, Holobar A, and Farina D. Multi-channel intramuscular and surface EMG decomposition by convolutive blind source separation. *J Neural Eng* 13: 026027, 2016a.
Negro F, Yavuz US, and Farina D. The human motor neuron pools receive a dominant slow-varying common synaptic input. *J Physiol* 594: 5491-5505, 2016b.
Norton JA, Bennett DJ, Knash ME, Murray KC, and Gorassini MA. Changes in sensory-evoked synaptic activation of motoneurons after spinal cord injury in man. *Brain* 131: 1478-1491, 2008.
Powers RK, and Heckman CJ. Contribution of intrinsic motoneuron properties to discharge hysteresis and its estimation based on paired motor unit recordings: a simulation study. *J Neurophysiol* 114: 184-198, 2015.
Powers RK, and Heckman CJ. Synaptic control of the shape of the motoneuron pool input-output function. *J Neurophysiol* 117: 1171-1184, 2017.
Powers RK, Nardelli P, and Cope TC. Estimation of the contribution of intrinsic currents to motoneuron firing based on paired motoneuron discharge records in the decerebrate cat. *J Neurophysiol* 100: 292-303, 2008.
Revill AL, and Fuglevand AJ. Effects of persistent inward currents, accommodation, and adaptation on motor unit behavior: a simulation study. *J Neurophysiol* 106: 1467-1479, 2011.
Revill AL, and Fuglevand AJ. Inhibition linearizes firing rate responses in human motor units: implications for the role of persistent inward currents. *J Physiol* 595: 179-191, 2017.
Stephenson JL, and Maluf KS. Dependence of the paired motor unit analysis on motor unit discharge characteristics in the human tibialis anterior muscle. *J Neurosci Methods* 198: 84-92, 2011.
Svirskis G, and Hounsgaard J. Depolarization-induced facilitation of a plateau-generating current in ventral horn neurons in the turtle spinal cord. *J Neurophysiol* 78: 1740-1742, 1997.
Udina E, D'Amico J, Bergquist AJ, and Gorassini MA. Amphetamine increases persistent inward currents in human motoneurons estimated from paired motor-unit activity. *J Neurophysiol* 103: 1295-1303, 2010.

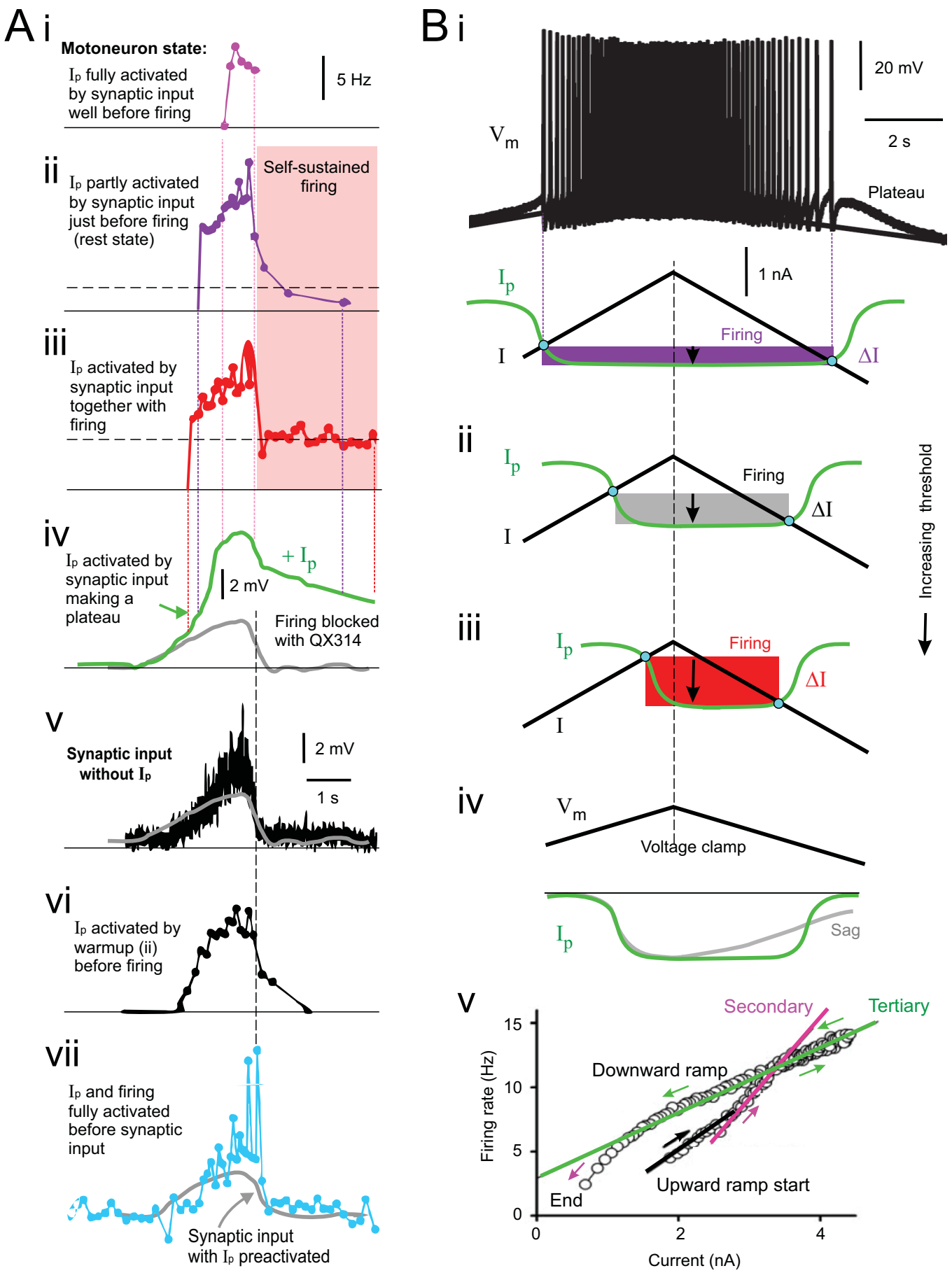

A

Torque

Recruitment threshold

10 %MVC

Rate [Hz]

Secondary range

Tertiary range

Sag

Asc Slope (1.36)

Dsc Slope (- 0.97)

MoD

Polynomial (R^2=0.75)

Start Rate

End Rate

Pulse amp.[au]

SIL (0.94)

2s

B

# of Units

10%

20%

30%

C

Accuracy (SIL)

10%

20%

30%

D

R^2 polynomial

MVC